Radio and EUV emission from MHD simulations of coronal jets

C. E. Alissandrakis, V. Archontis,
S. Patsourakos, K. Moraitis, J. Zhuleku, A. Nindos
University of Ioannina, Greece

Outline

- Introduction
- The simulations
- Computation of microwave emission
- Computation of EUV emission
- Comparison with observations

My favorite jet (TRACE images)

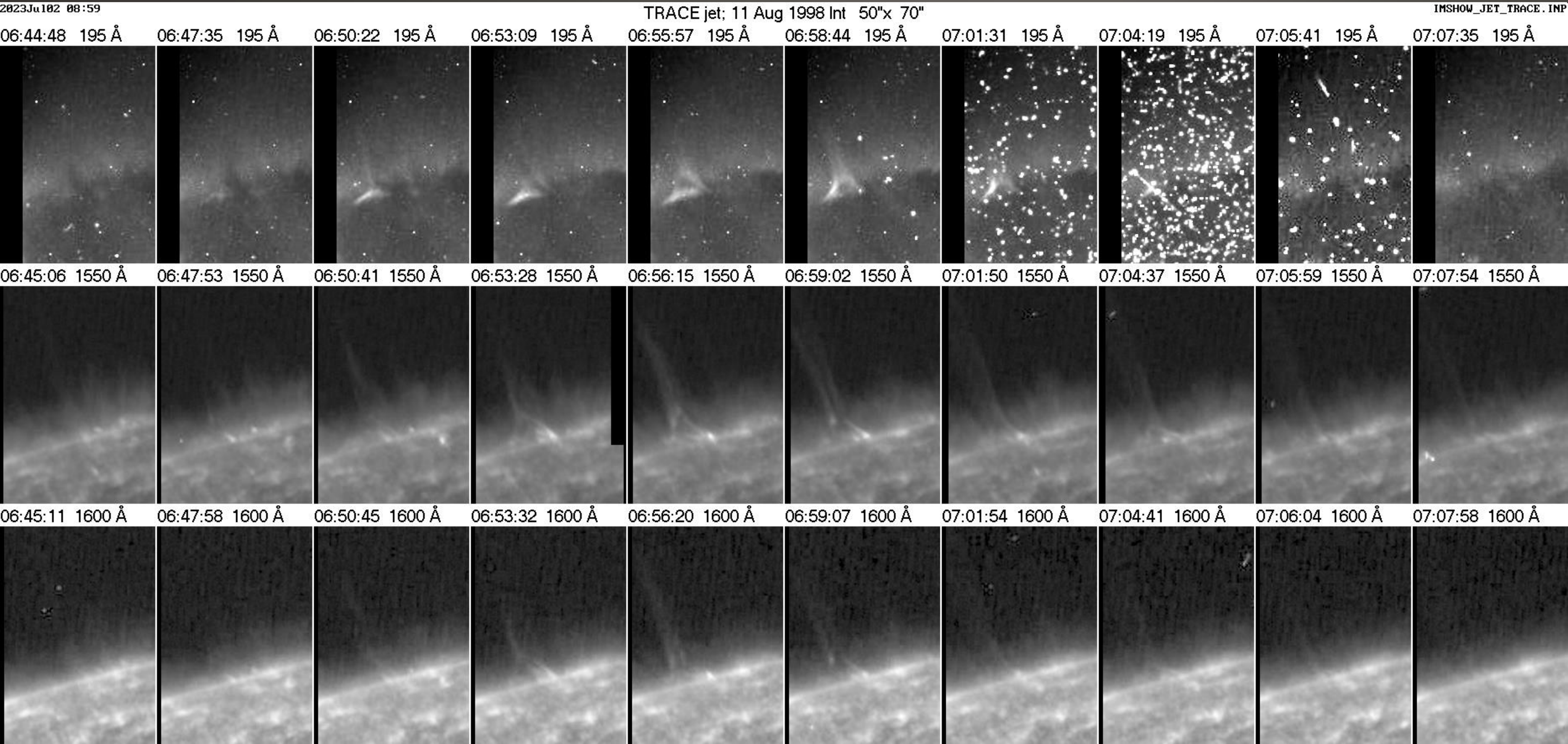

'Standard' & 'blowout' jets: schematic models

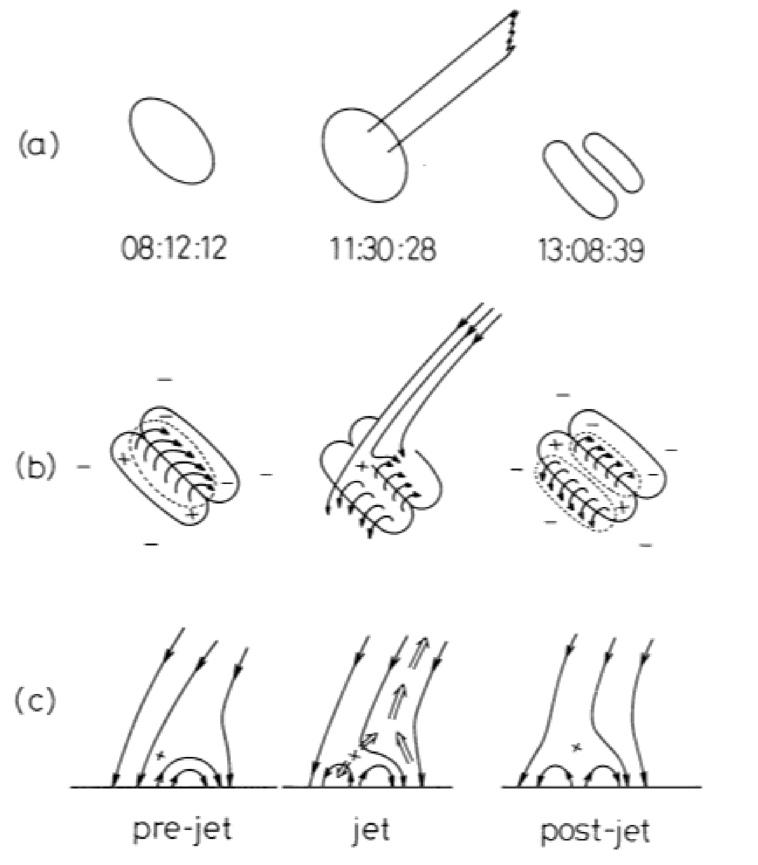

Fig. 5. Schematic picture of the possible physical situation of the 1991 November 12 jet. (a) Cartoons of the SXT image of the active regions and jets for pre-jet, jet, and post-jet stages. (b) Magnetogram data and the birds-eye view of the inferred magnetic field line configuration. (c) Side view of the magnetic reconnection occurring between the emerging flux and the pre-existing coronal field.

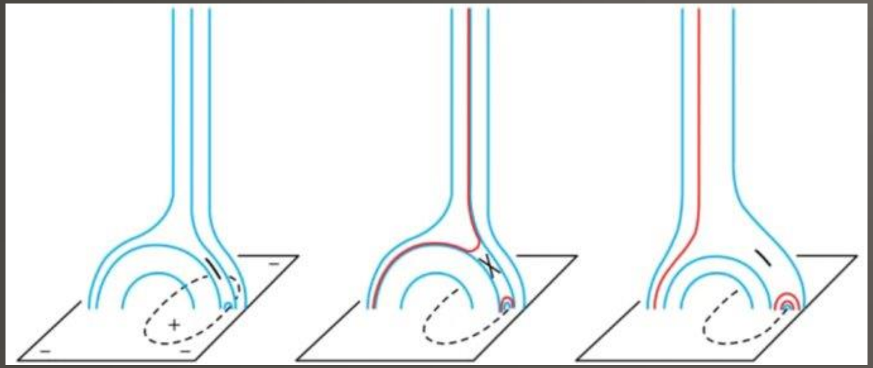

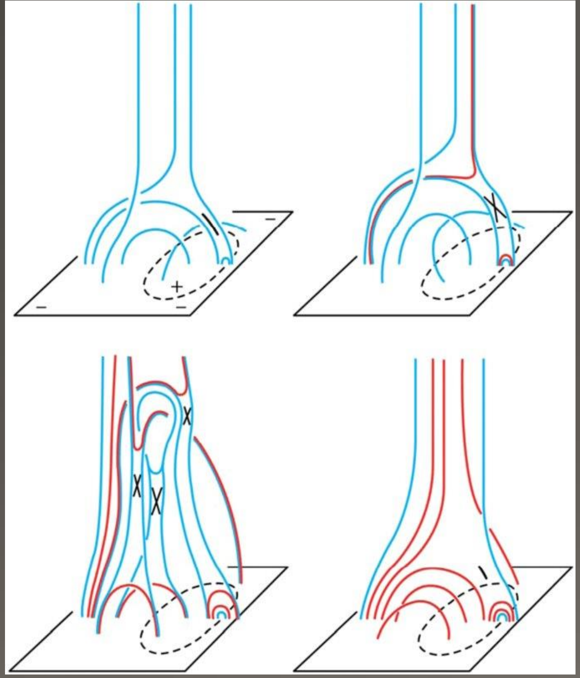

'Standard' jets.

- Emerging arch + 'open' ambient field.
- 'External' reconnection.
- X-ray jet + 'bright' point (arcade).
- Little or no emission in cooler lines.

'Blowout' jets.

- Eruption of the field.
- 'External' & 'Internal' reconnection.
- Wider jet channel.
- Hot and cool emission.
- Brightening on arcades.

Shibata et.al. (1992).

Moore et al. 2010, 2013, Sterling et al. 2010, Liu et al. 2011, Shen et al. 2012, etc.

The simulations

- Basic equations
- Background atmosphere & geometry
- Results
- See Archontis & Hood, 2013; Chouliaras et al., 2023

Numerical experiments: MHD equations

$$\frac{\partial \rho}{\partial t} = -\nabla \cdot (\rho \boldsymbol{u}),$$
$$\frac{\partial (\rho \boldsymbol{u})}{\partial t} = -\nabla \cdot \left(\rho \boldsymbol{u} \otimes \boldsymbol{u} + \underline{\underline{\tau}}\right) - \nabla p + \rho \boldsymbol{g} + \frac{\boldsymbol{J}}{c} \times \boldsymbol{B},$$
$$\frac{\partial e}{\partial t} = -\nabla \cdot (e\boldsymbol{u}) - p \nabla \cdot \boldsymbol{u} + Q_{\mathrm{Joule}} + Q_{\mathrm{visc}},$$

Continuity,

momentum and

energy conservation

$$\frac{\partial \boldsymbol{B}}{\partial t} = -c \nabla \times \boldsymbol{E},$$
$$\boldsymbol{E} = -\frac{\boldsymbol{u}}{c} \times \boldsymbol{B} + \eta \frac{\boldsymbol{J}}{c^2},$$
$$\boldsymbol{J} = \frac{c}{4\pi} \nabla \times \boldsymbol{B},$$

Faraday,

Ohm and

Ampere’s law.

$$p = \rho T \frac{\mathcal{R}}{\tilde{\mu}},$$

EOS.

Thermodynamics: ideal gas, no heat conduction, no radiative cooling.

Initial conditions: atmosphere and magnetic field

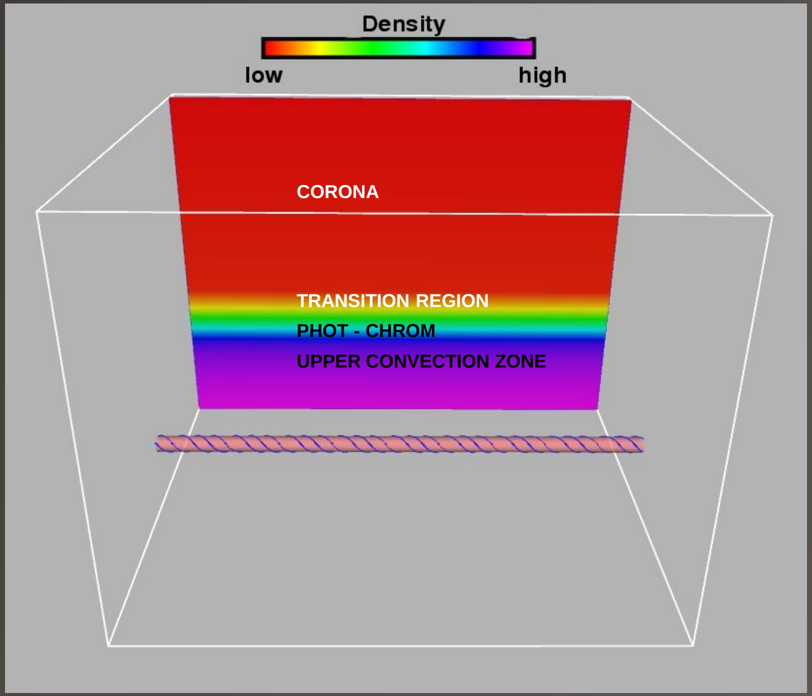

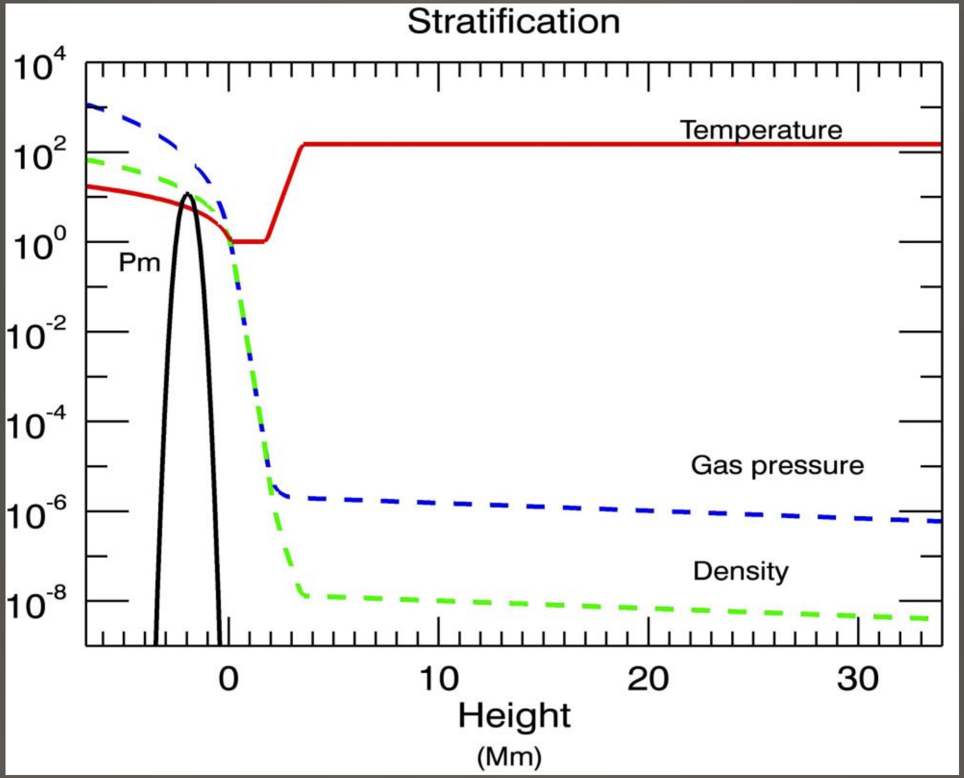

- Stratified (plane-parallel) atmosphere.
- Magnetic flux tube (twisted).
- Density deficit → buoyancy.
- Ambient magnetic field.

- Atmosphere, magnetic field(s).
- Large density and pressure contrast.
- Hydrostatic equilibrium.
- 3D resistive MHD (Lare3d code).

The simulation

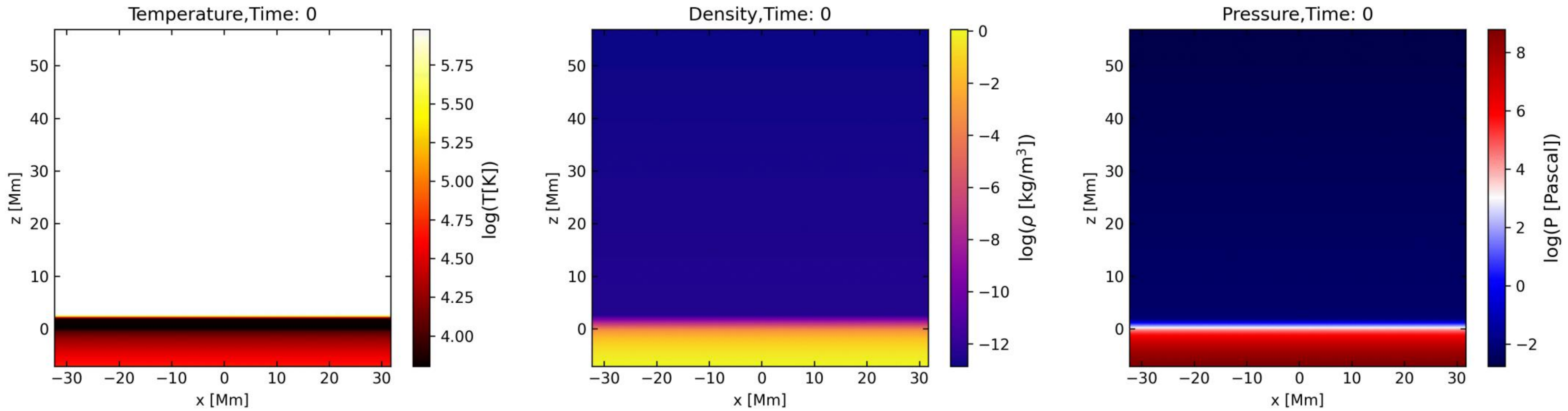

Temperature

Density

Pressure

Two jet phases:

- The first is a “regular” jet that forms at t=30 when the emerging field reconnects with the ambient field
- The second appears at t=50+ after the formation of a flux rope which subsequently reconnects with the ambient field and erupts creating a “blowout” jet

Computation of radio emission

- Used temperature & density computed with the simulation
- Thermal bremsstrahlung only
- No energetic particles
- Ignored magnetic field
- 400x400x400 grid, step 0.18 Mm
- Time step 86.9 s
- Computed images on the xy, xz and yz planes at 17 & 300 GHz
- Computed flux as a function of time

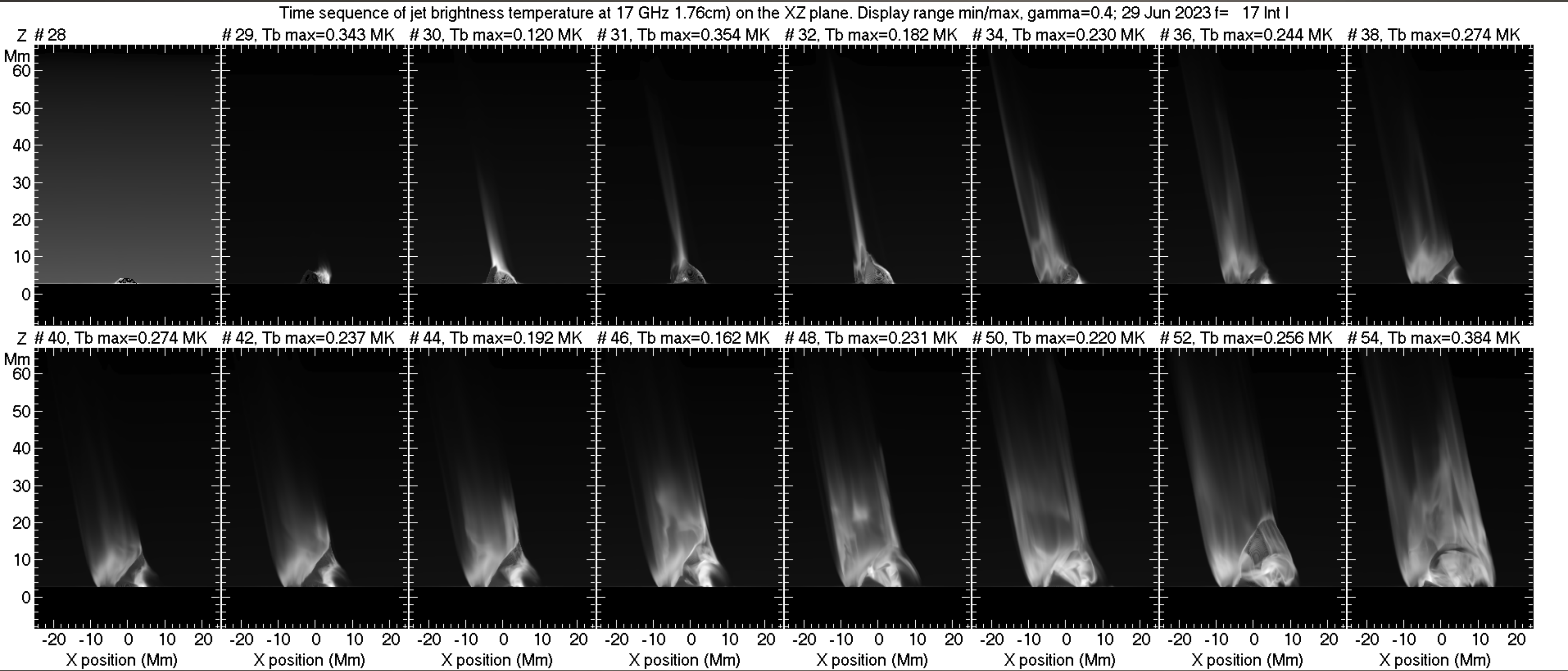
Time sequence of jet brightness temperature at 17 GHz 1.76cm) on the XZ plane. Display range min/max, gamma=0.4; 29 Jun 2023 f= 17 Int I
Z Mm
28
29, Tb max=0.343 MK
30, Tb max=0.120 MK
31, Tb max=0.354 MK
32, Tb max=0.182 MK
34, Tb max=0.230 MK
36, Tb max=0.244 MK
38, Tb max=0.274 MK
40, Tb max=0.274 MK
42, Tb max=0.237 MK
44, Tb max=0.192 MK
46, Tb max=0.162 MK
48, Tb max=0.231 MK
50, Tb max=0.220 MK
52, Tb max=0.256 MK
54, Tb max=0.384 MK
X position (Mm)

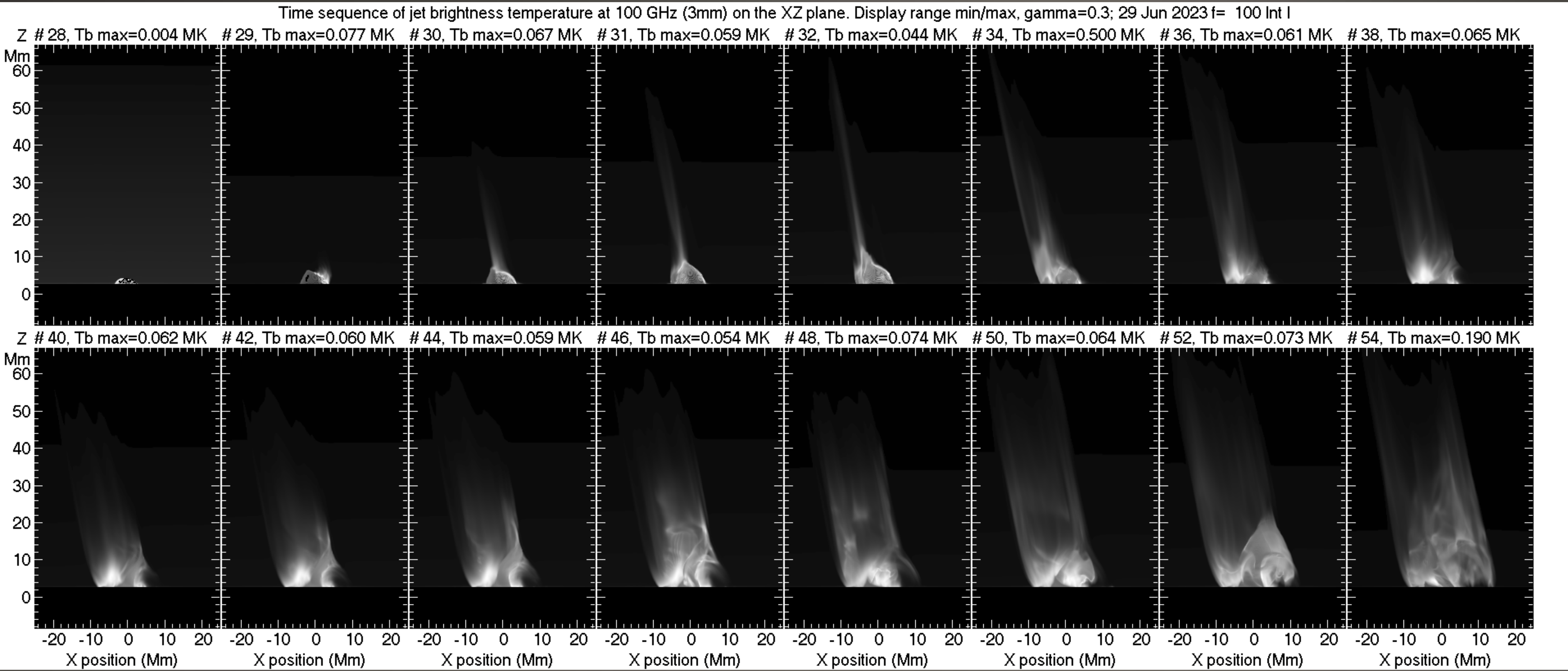
Time sequence of jet brightness temperature at 100 GHz (3mm) on the XZ plane. Display range min/max, gamma=0.3; 29 Jun 2023 f= 100 Int I
28, Tb max=0.004 MK
29, Tb max=0.077 MK
30, Tb max=0.067 MK
31, Tb max=0.059 MK
32, Tb max=0.044 MK
34, Tb max=0.500 MK
36, Tb max=0.061 MK
38, Tb max=0.065 MK
40, Tb max=0.062 MK
42, Tb max=0.060 MK
44, Tb max=0.059 MK
46, Tb max=0.054 MK
48, Tb max=0.074 MK
50, Tb max=0.064 MK
52, Tb max=0.073 MK
54, Tb max=0.190 MK
Z Mm
X position (Mm)

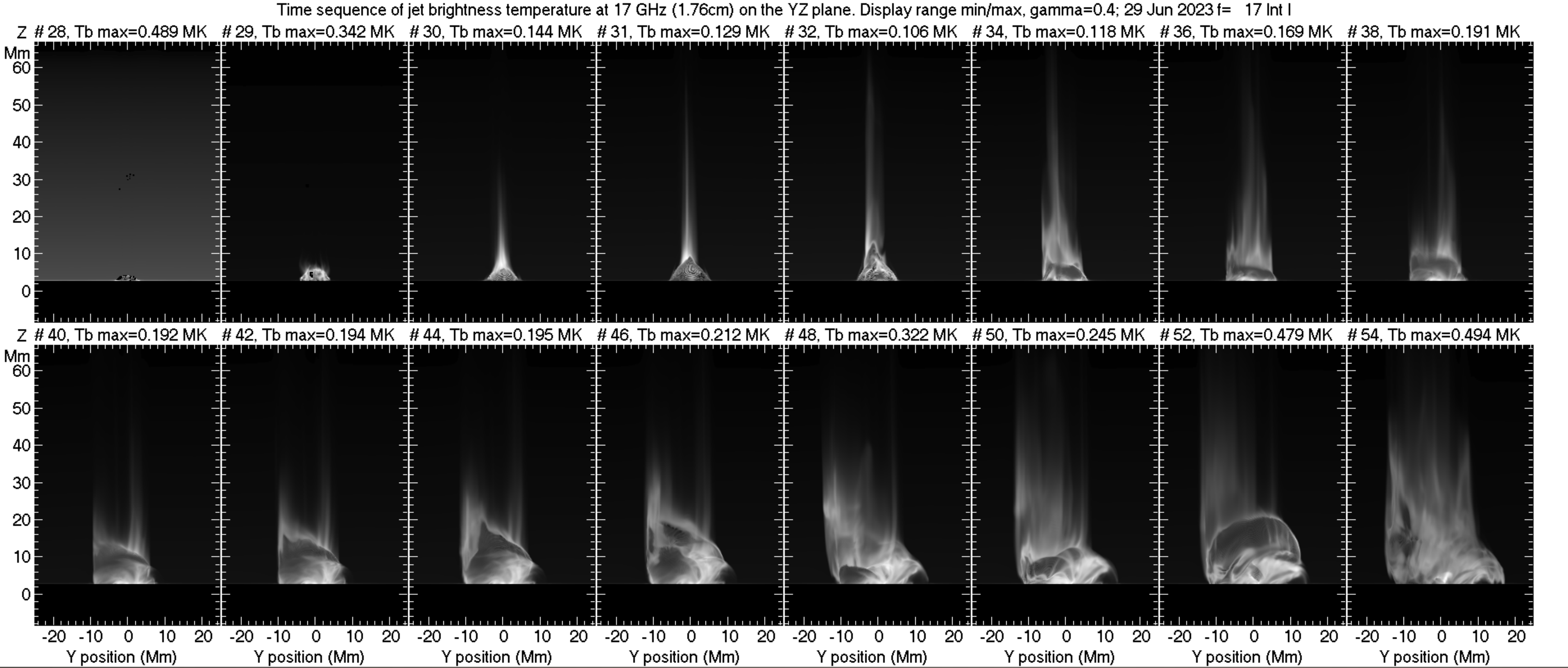
Time sequence of jet brightness temperature at 17 GHz (1.76cm) on the YZ plane. Display range min/max, gamma=0.4; 29 Jun 2023 f= 17 Int I
28, Tb max=0.489 MK
29, Tb max=0.342 MK
30, Tb max=0.144 MK
31, Tb max=0.129 MK
32, Tb max=0.106 MK
34, Tb max=0.118 MK
36, Tb max=0.169 MK
38, Tb max=0.191 MK
40, Tb max=0.192 MK
42, Tb max=0.194 MK
44, Tb max=0.195 MK
46, Tb max=0.212 MK
48, Tb max=0.322 MK
50, Tb max=0.245 MK
52, Tb max=0.479 MK
54, Tb max=0.494 MK
Z Mm
Y position (Mm)

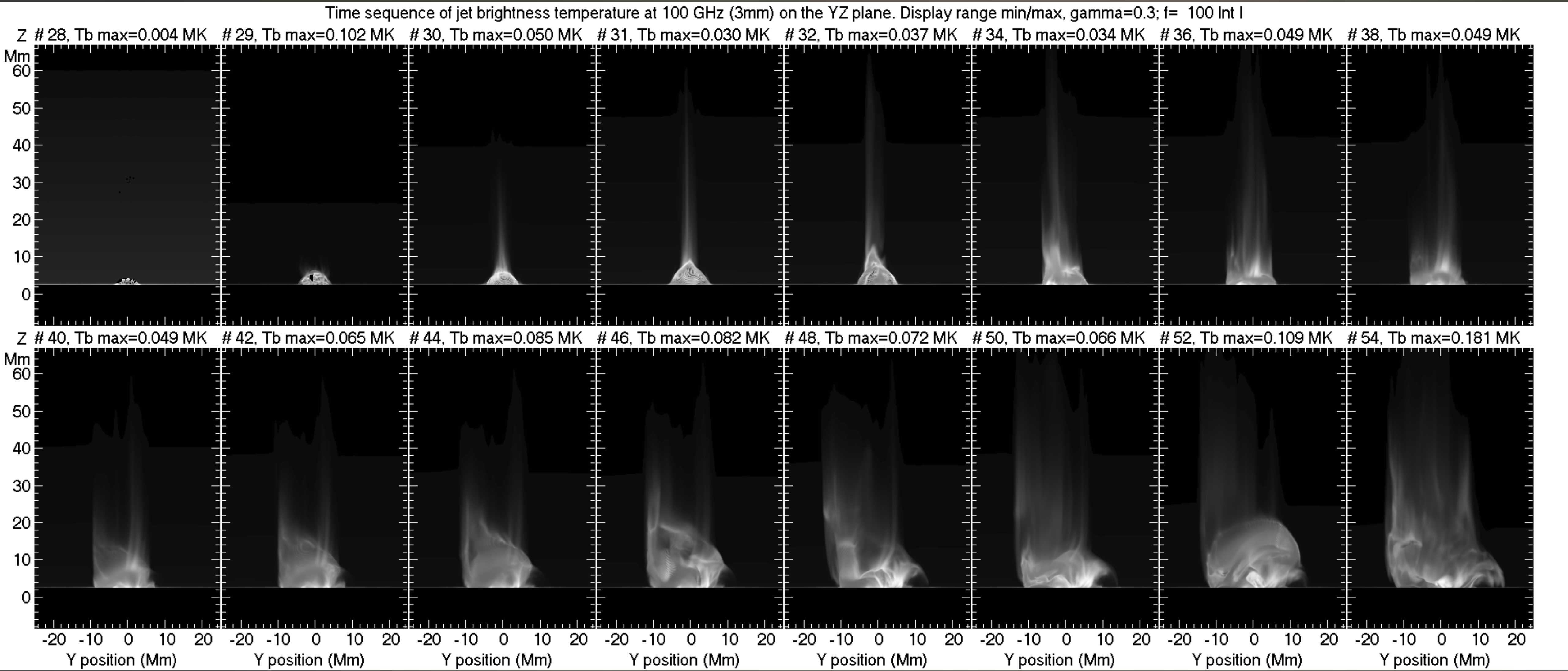
Time sequence of jet brightness temperature at 100 GHz (3mm) on the YZ plane. Display range min/max, gamma=0.3; f= 100 Int I
28, Tb max=0.004 MK
29, Tb max=0.102 MK
30, Tb max=0.050 MK
31, Tb max=0.030 MK
32, Tb max=0.037 MK
34, Tb max=0.034 MK
36, Tb max=0.049 MK
38, Tb max=0.049 MK
40, Tb max=0.049 MK
42, Tb max=0.065 MK
44, Tb max=0.085 MK
46, Tb max=0.082 MK
48, Tb max=0.072 MK
50, Tb max=0.066 MK
52, Tb max=0.109 MK
54, Tb max=0.181 MK
Z
Mm
Y position (Mm)

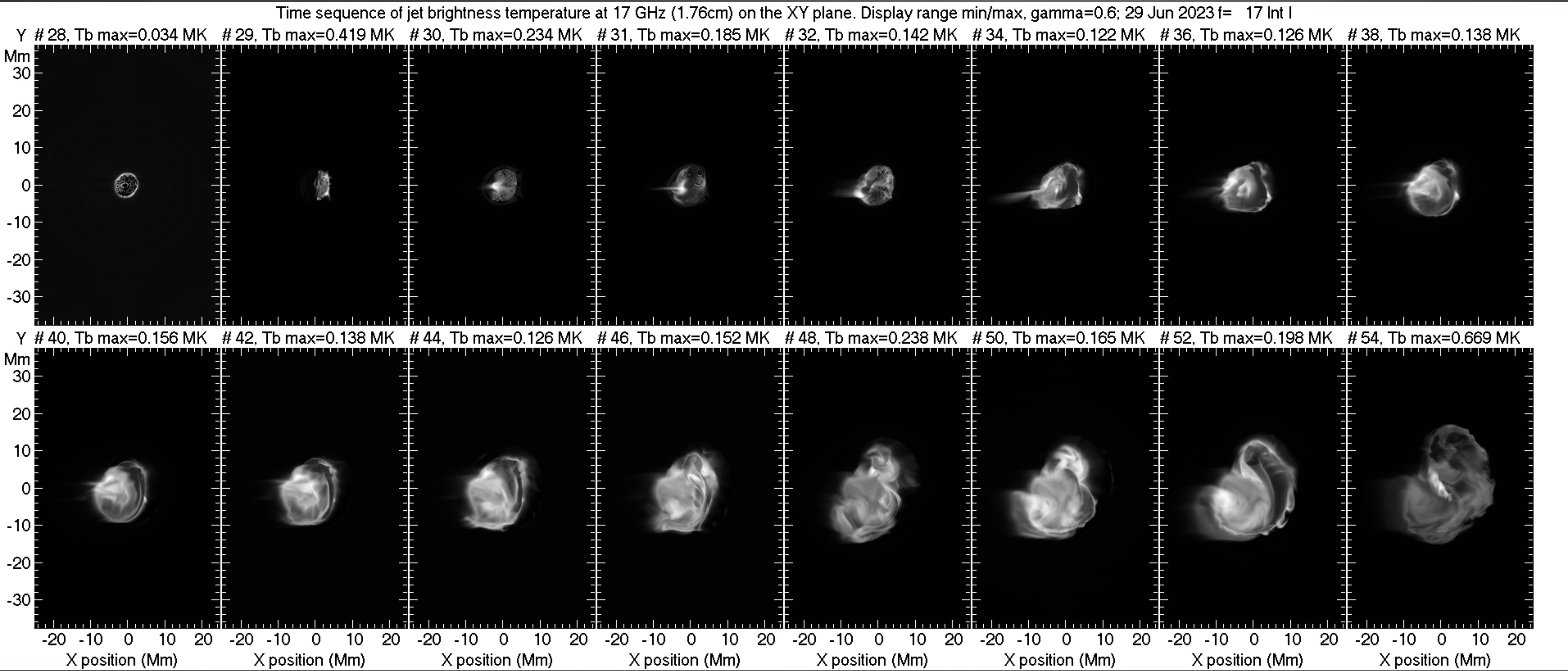
Time sequence of jet brightness temperature at 17 GHz (1.76cm) on the XY plane. Display range min/max, gamma=0.6; 29 Jun 2023 f= 17 Int I
28, Tb max=0.034 MK
29, Tb max=0.419 MK
30, Tb max=0.234 MK
31, Tb max=0.185 MK
32, Tb max=0.142 MK
34, Tb max=0.122 MK
36, Tb max=0.126 MK
38, Tb max=0.138 MK
40, Tb max=0.156 MK
42, Tb max=0.138 MK
44, Tb max=0.126 MK
46, Tb max=0.152 MK
48, Tb max=0.238 MK
50, Tb max=0.165 MK
52, Tb max=0.198 MK
54, Tb max=0.669 MK
Y Mm
X position (Mm)

Time sequence of jet brightness temperature at 100 GHz (3mm) on the XY plane. Display range min/max, gamma=0.6; 29 Jun 2023 f= 100 Int I

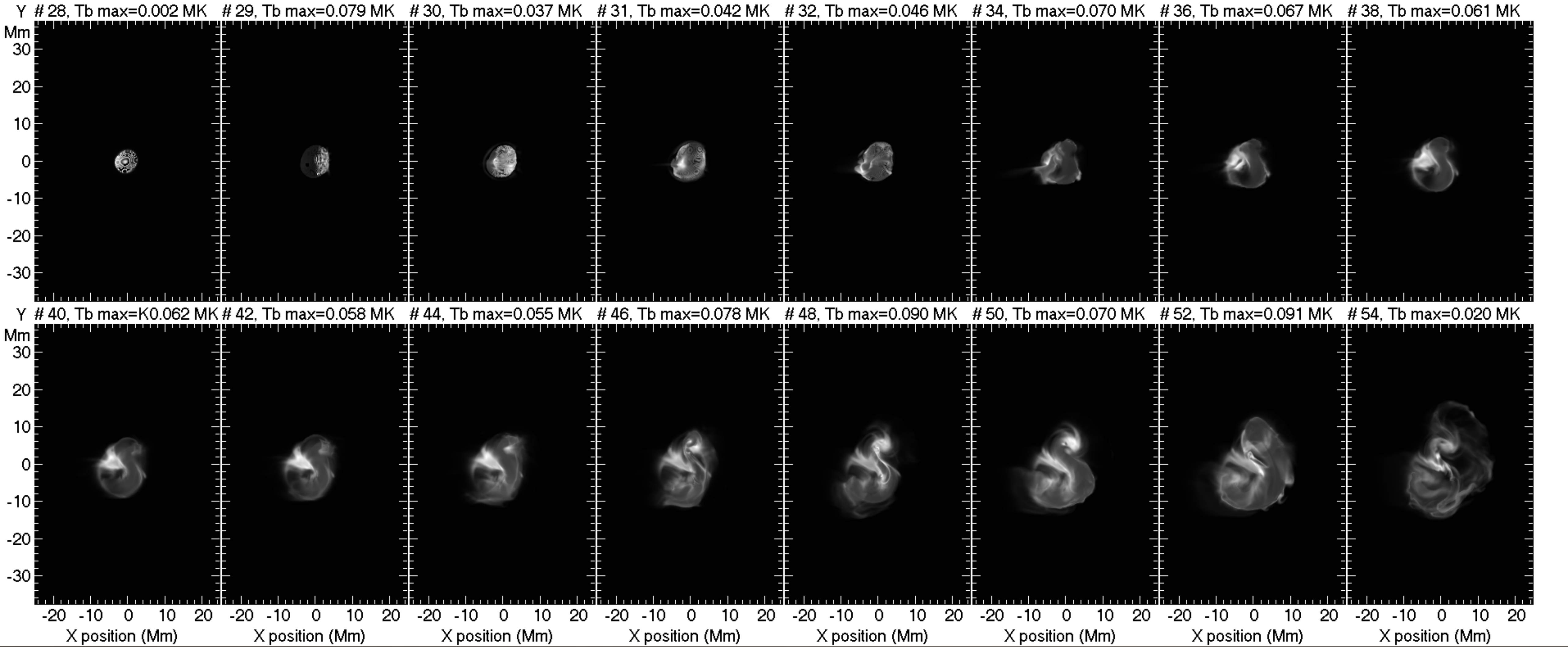

Radio flux as a function of time

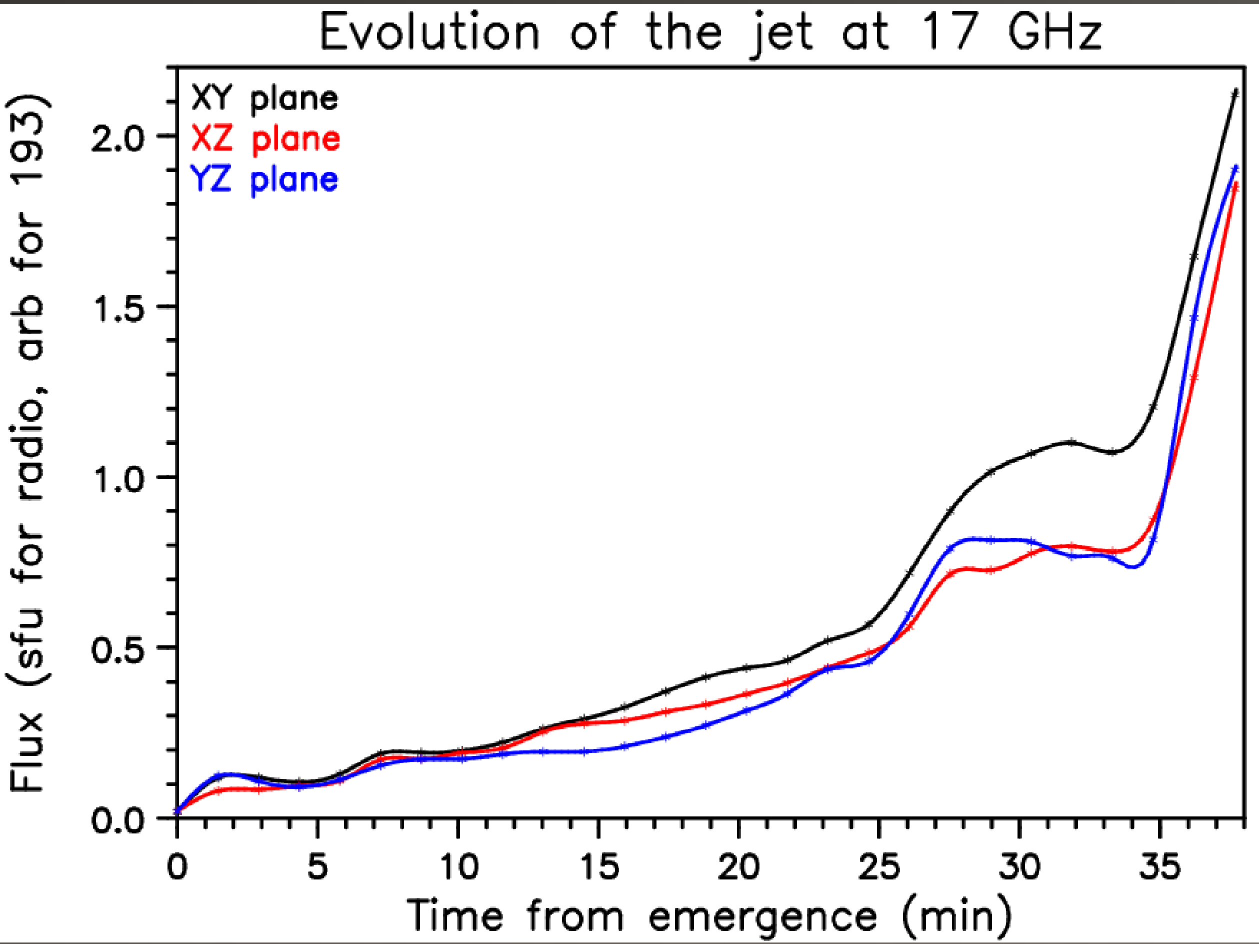

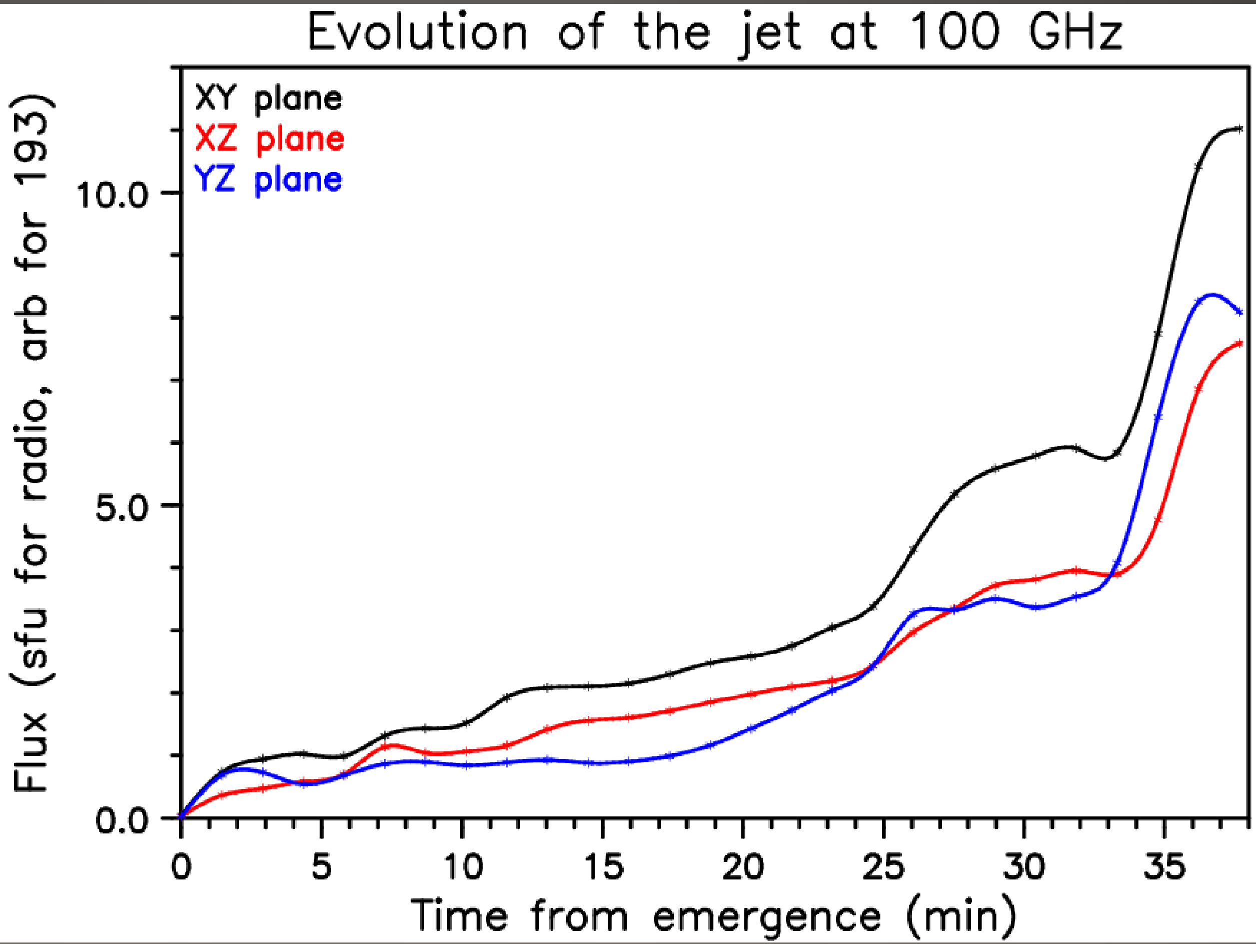

Computation of EUV emission

- Used the temperature response functions of various AIA EUV channels and the temperature and density results from the MHD simulations and calculated EUV emissivities at each voxel of the data-cubes
- Assuming optically-thin emission integrated the emissivity cubes from three different orthogonal to the simulation grid viewpoints
- The resulting images are in the native spatial binning (180 km) of the MHD simulation; no absorption from neutral Hydrogen was considered

Side views of the jets

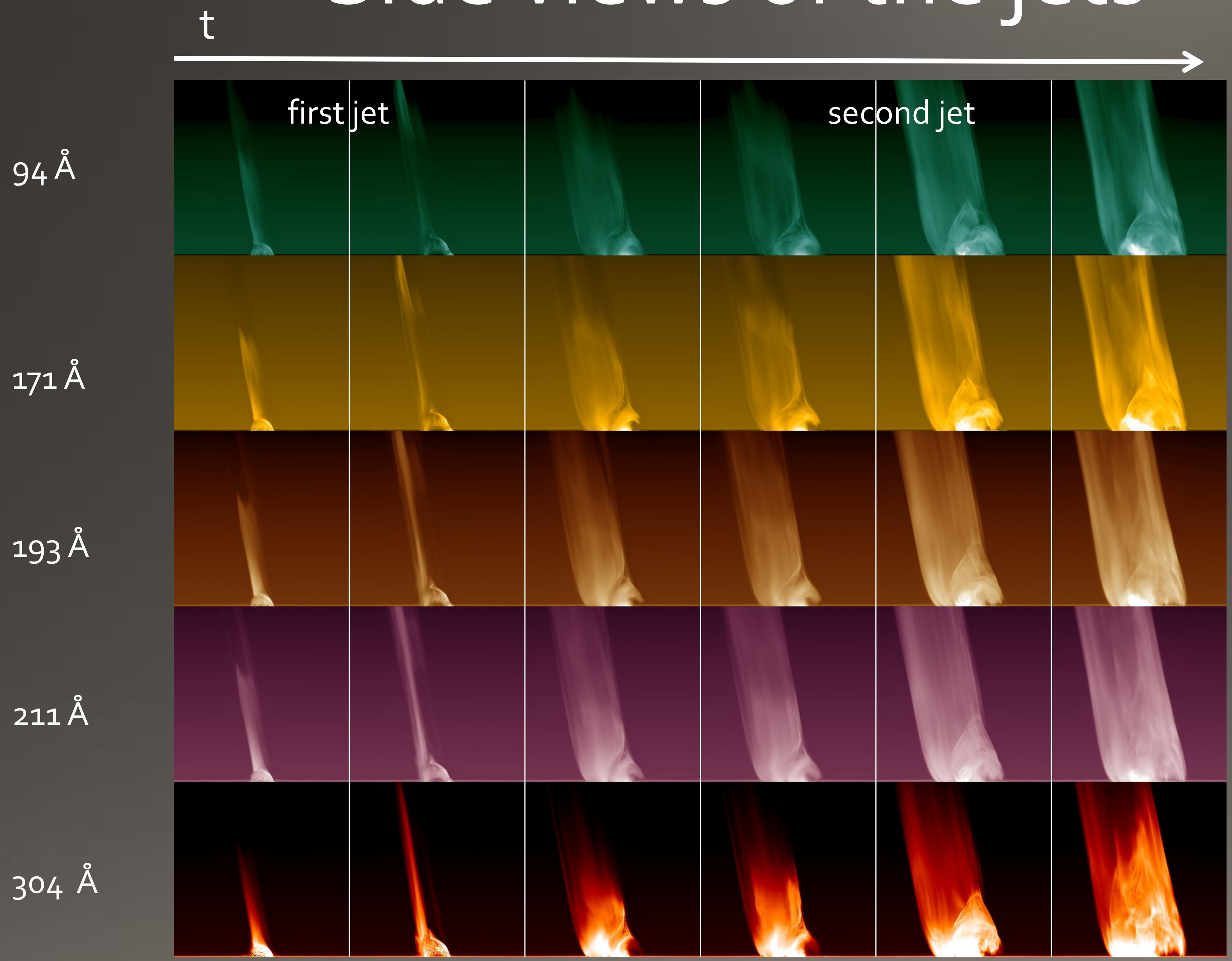

First jet: standard
Second jet: blowout.

Similar morphologies in the different AIA channels. Plasmas at mainly 1-2 MK.

The first jet has smaller base and a narrower spire than the second jet.

Top views of the jets

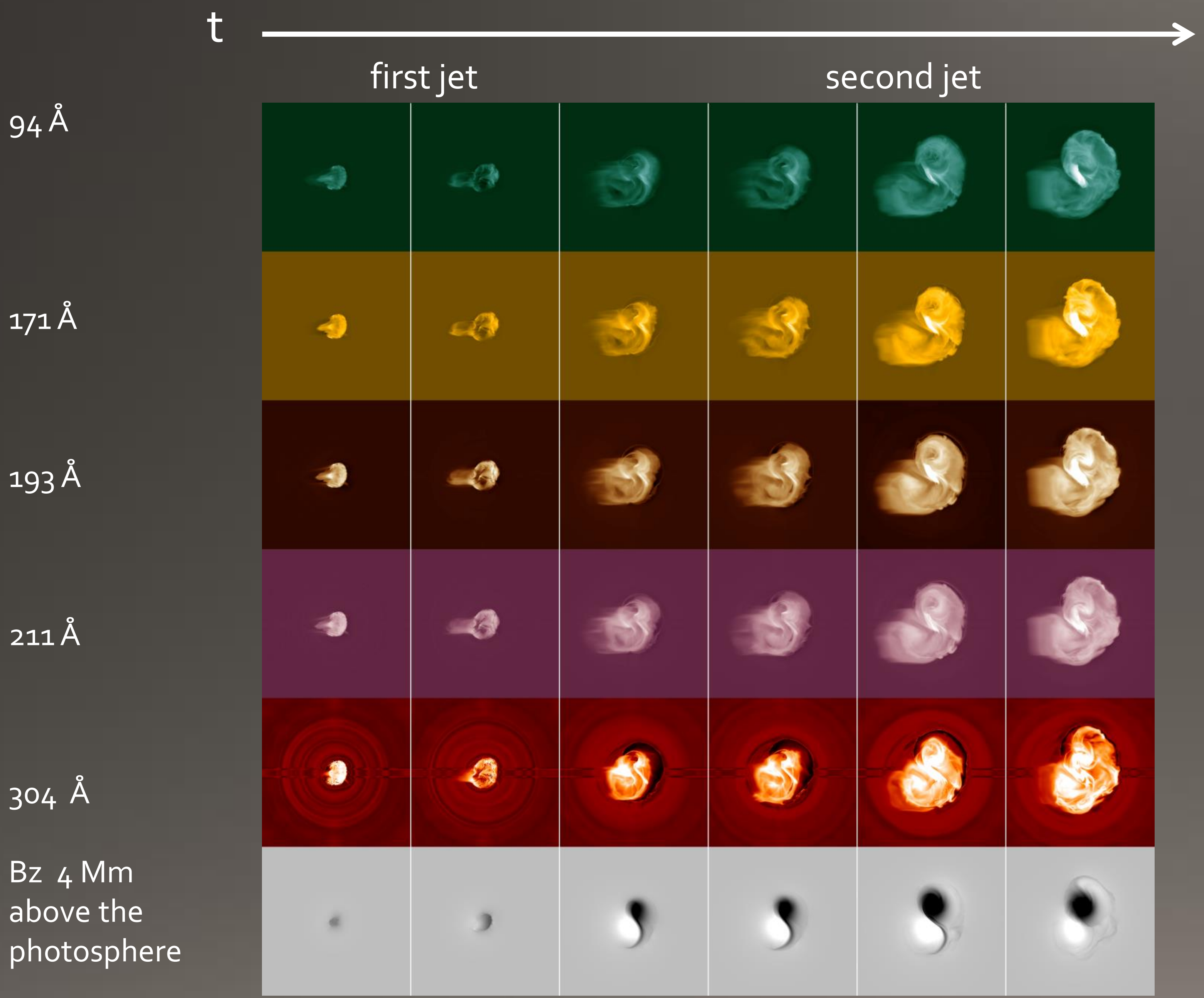

Radio & AIA intensity

Image contrast adjusted for best visibility

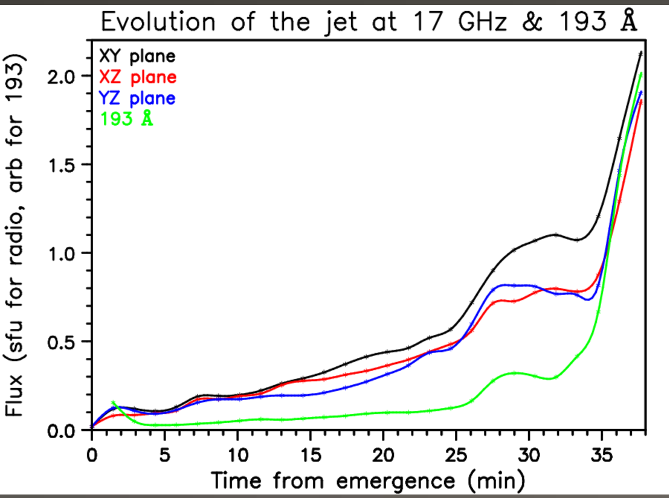

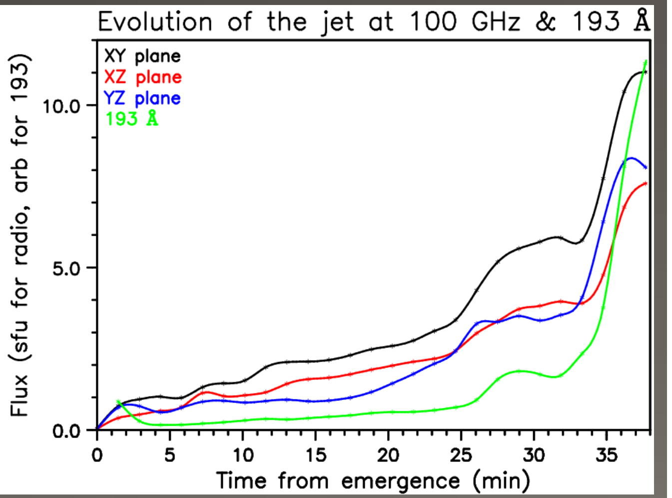

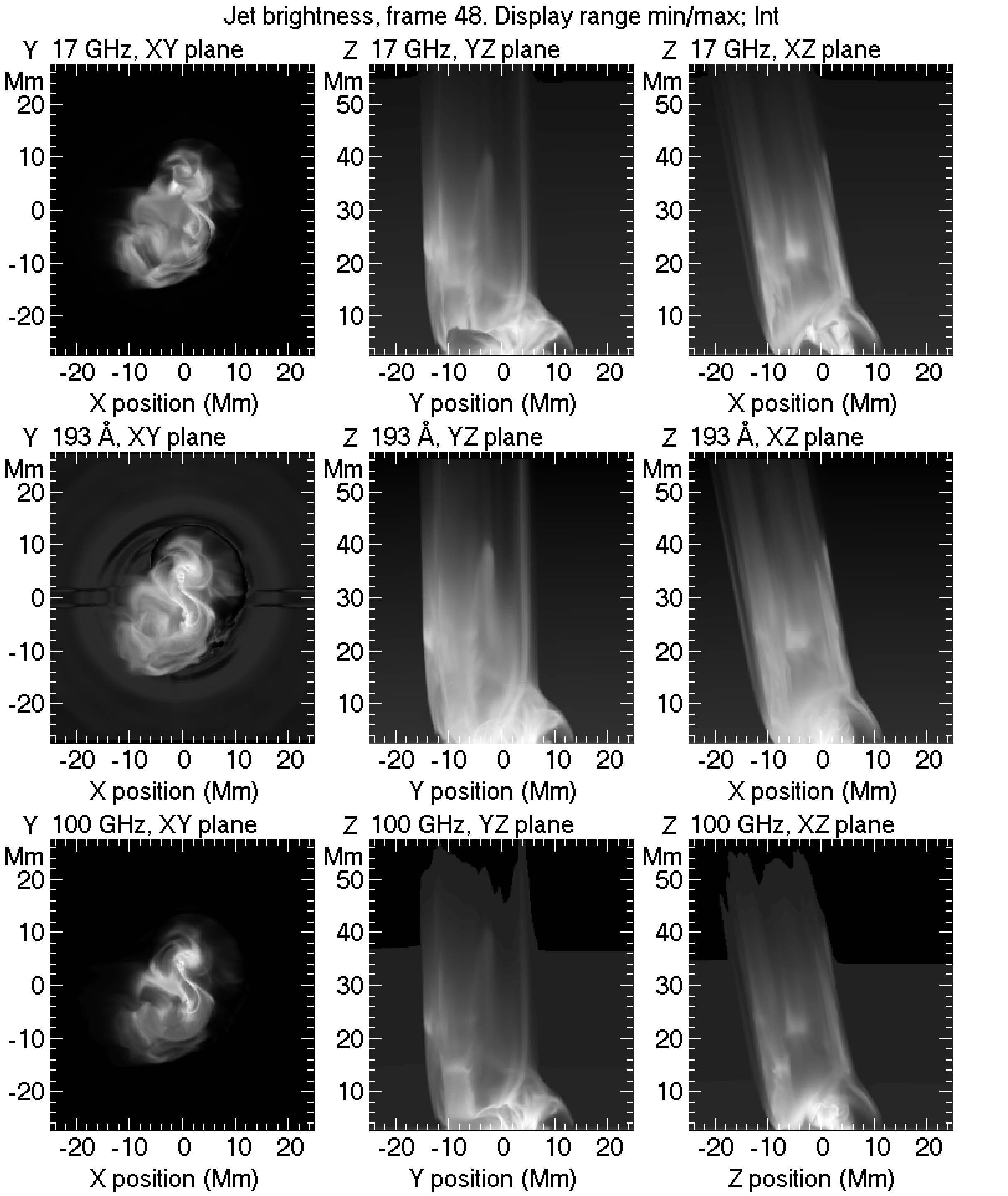

Observations: NoRH (17 GHz)

- Kundu, Shibasaki, & Nitta 1997
- Kundu et al., 1999
- Kaltman et al., 2021

Kundu et al., 1997 (I)

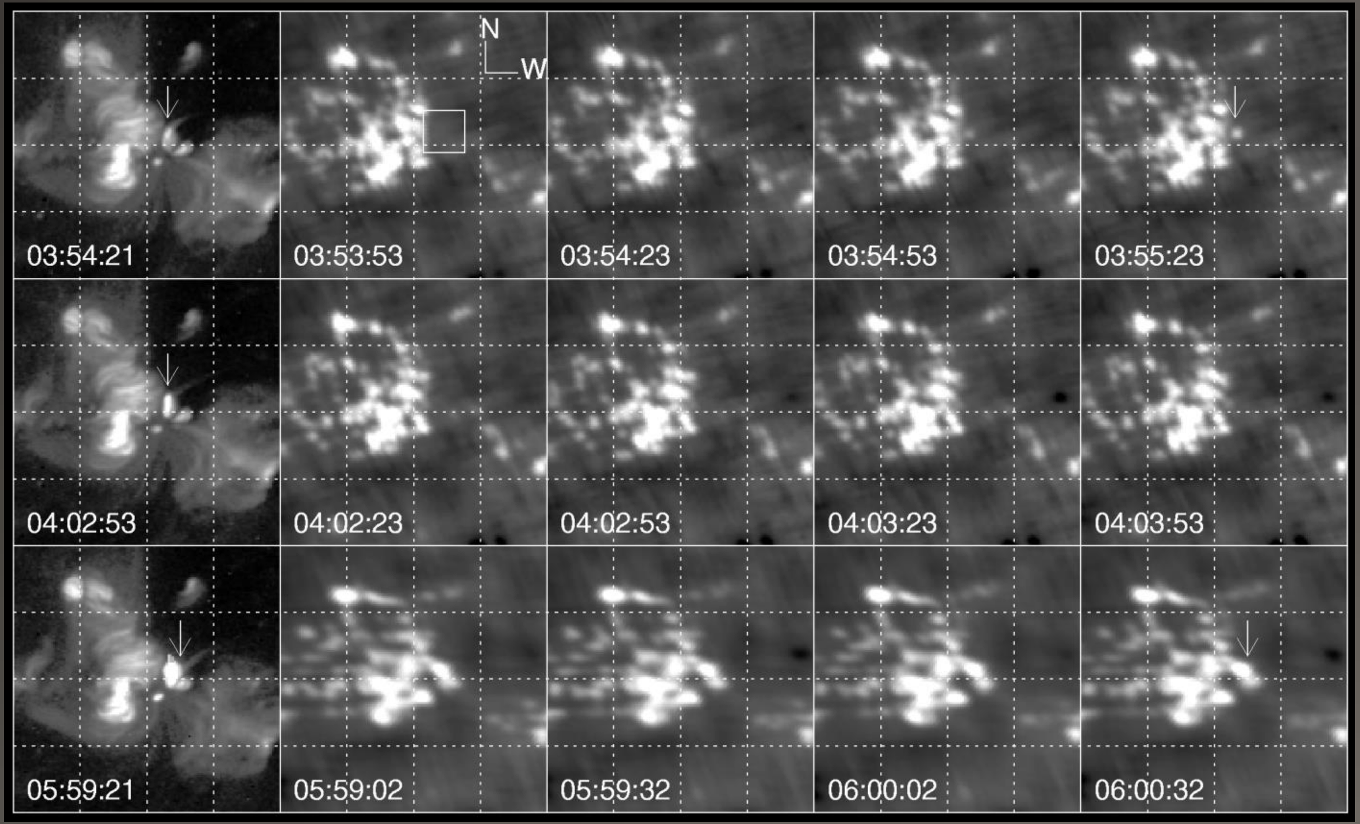

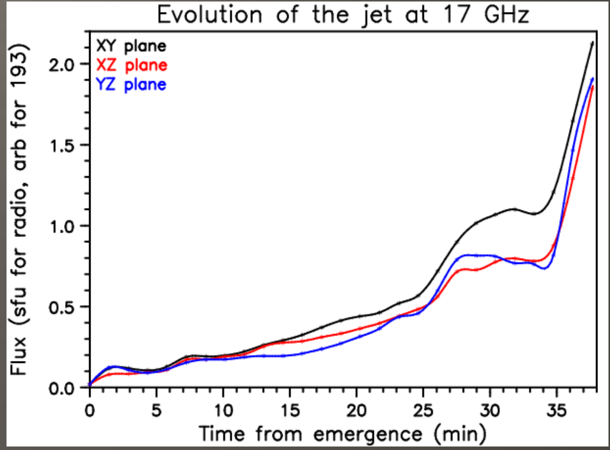

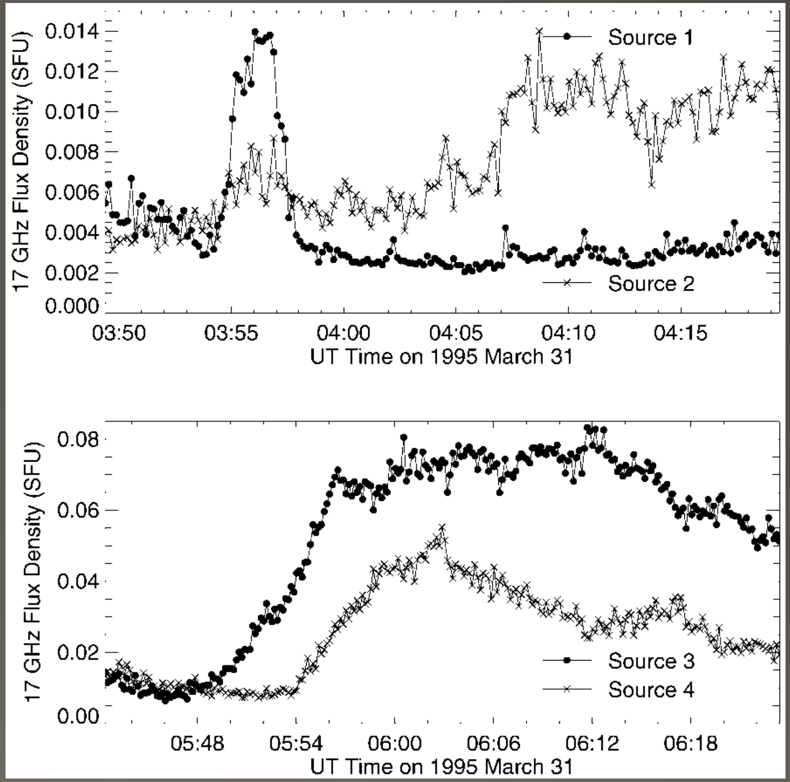

Kundu et al., 1997 (II)

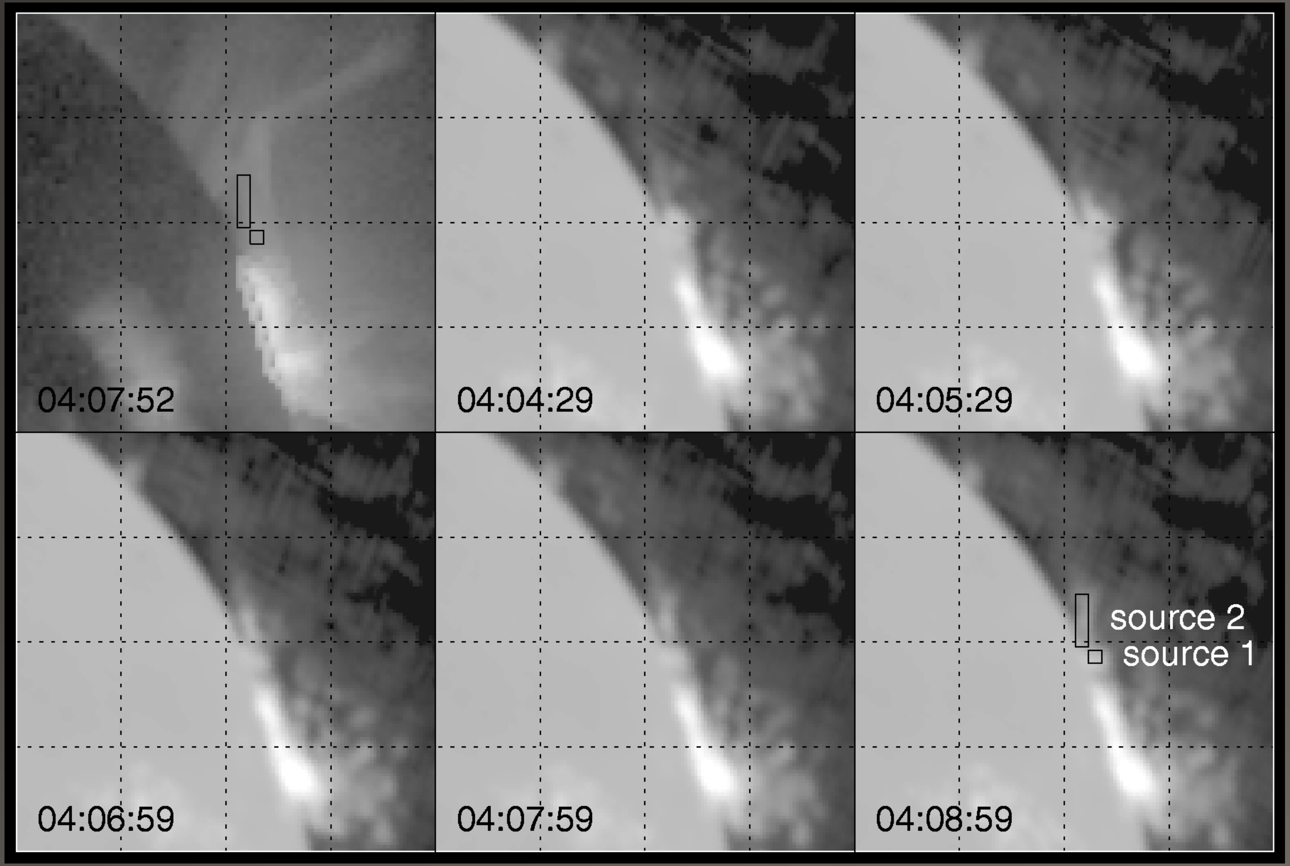

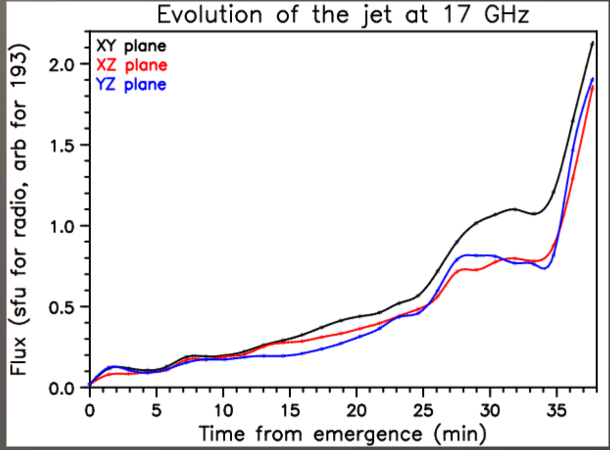

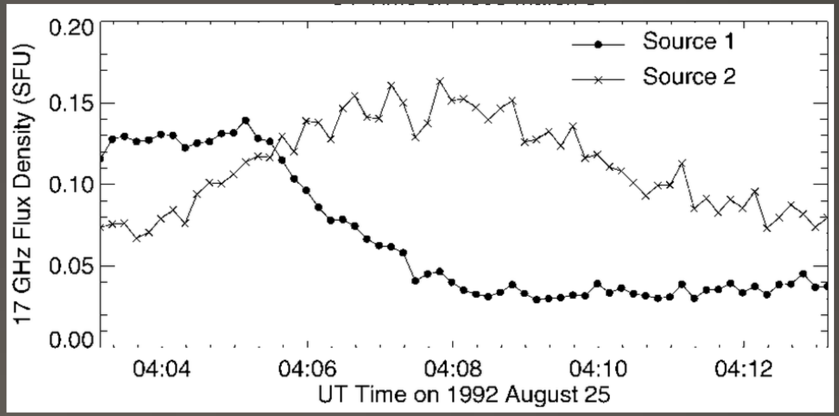

Kundu et al. 1999

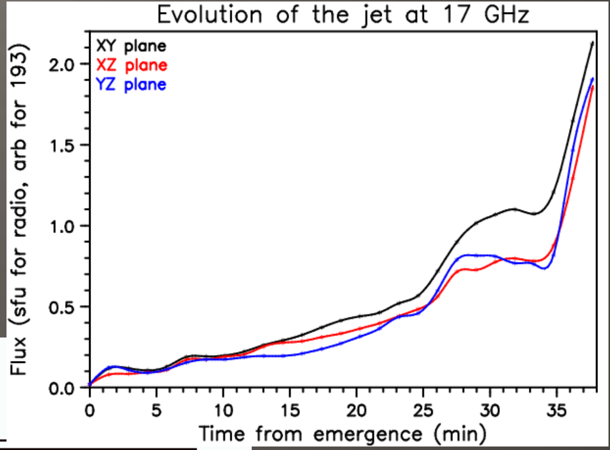

X-Ray Jets and 17 GHz Radio Emission

Date	SXT Start (UT)	SXT End (UT)	SXT Base Enhancement	17 GHz Emission	Radio Flux (sfu)	rms Noise (sfu)
1992 Jul 22[a]	01:16	>02:15	Yes	Base/both sides	0.18/0.22	0.017
1992 Aug 17	01:28	>02:04	No	Base	0.09	0.011
1993 Feb 09[a]	03:59	>04:16	Yes	Base/lower part	0.35/0.20	0.017
1993 Apr 21a	01:10	>01:28	No	Base/lower part	0.11	0.019
1993 Apr 21b[a]	01:10	>01:36	Yes	Base	0.15	0.020
1993 Jul 12	03:11	03:11	No	No	...	0.016
1993 Sep 24[a]	04:56	04:58	Yes	Base	0.08	0.021
1993 Oct 02	04:10	04:17	Yes	No	...	0.014
1993 Oct 03	03:04	>03:34	Yes	Base	0.12	0.011
1994 Jan 05a[a]	03:03	03:12	Yes	Base	0.09	0.018
1994 Jan 05b	03:01	03:28	No	No	...	0.019
1994 Jan 06[a]	02:00	>02:02	Yes	Base	0.065	0.017
1994 Jul 13	00:57	01:04	No	No	...	0.012
1994 Dec 22a	01:58	02:02	Yes	Base/lower part	0.11	0.013
1994 Dec 22b	02:27	>02:29	Yes	Base/lower part	0.15	0.015
1994 Dec 22c	03:31	03:48	Yes	Base/lower part	0.08	0.013
1994 Dec 22d	05:25	05:43	Yes	Base/lower part	0.09	0.016
1994 Dec 26	01:38	02:08	Yes	Base/lower part	0.13	0.017
1995 Mar 31	05:55	06:18	Yes	Base	0.09	0.009

Kaltman 007, June 27, 2010

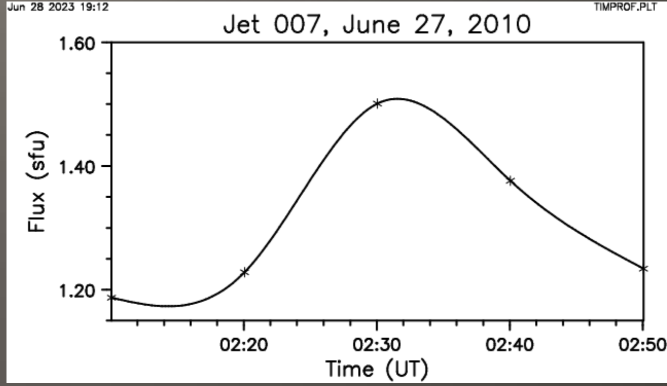

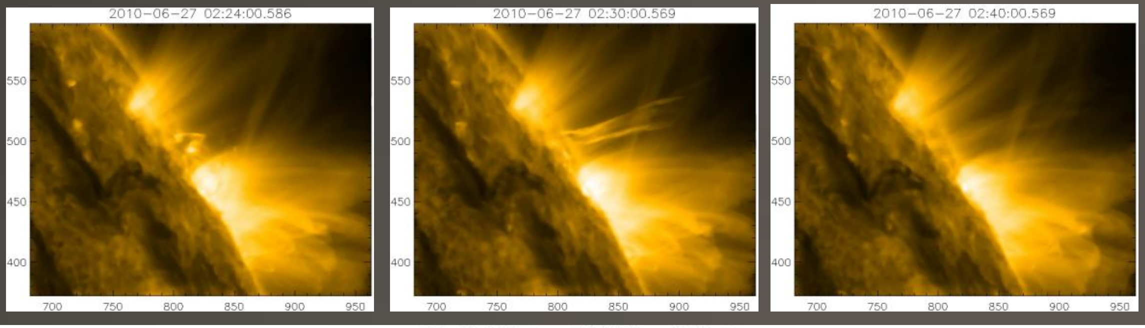

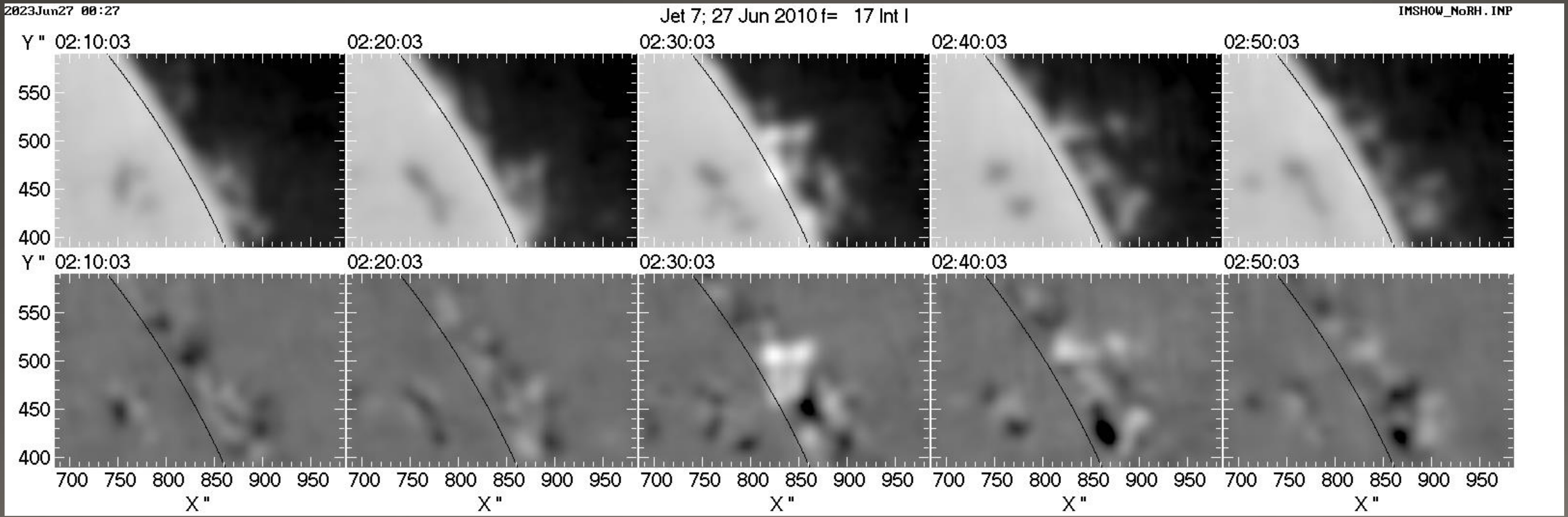

Kaltman 097, Jan 29, 2013

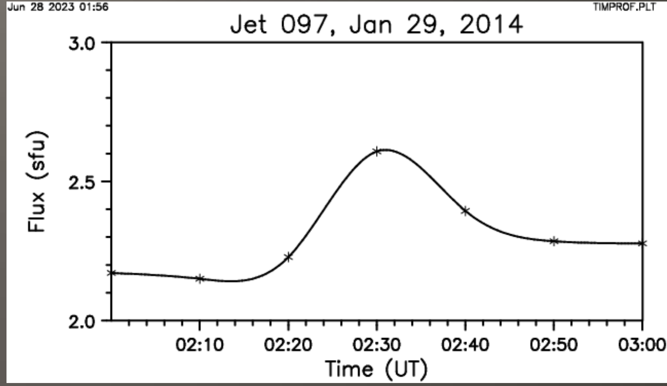

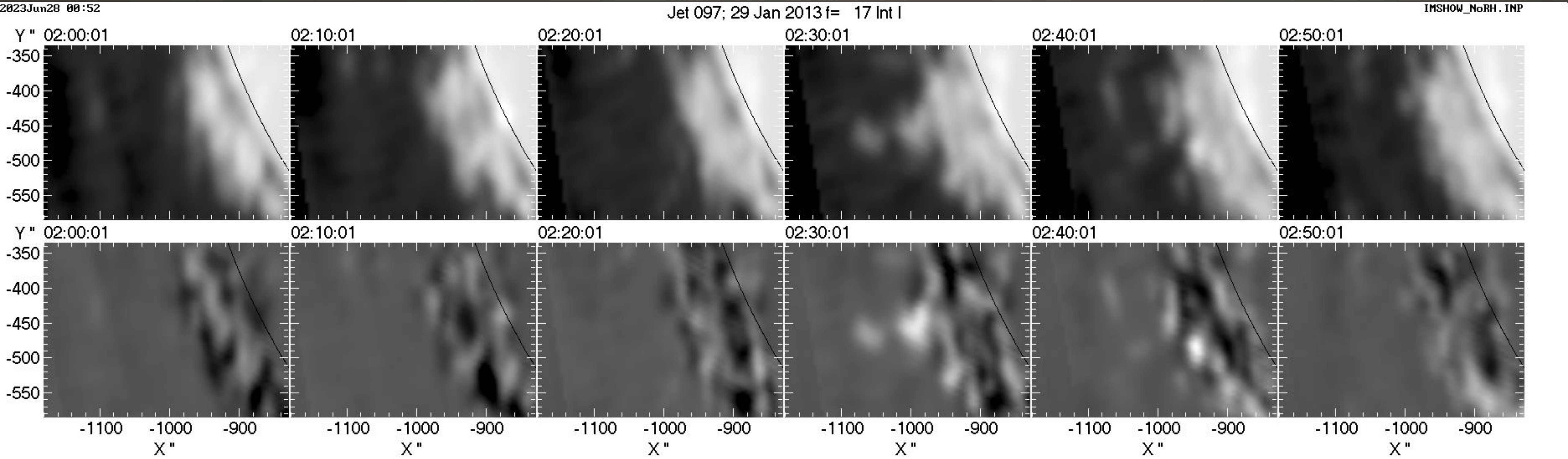

Kaltman 145, Oct 13, 2014

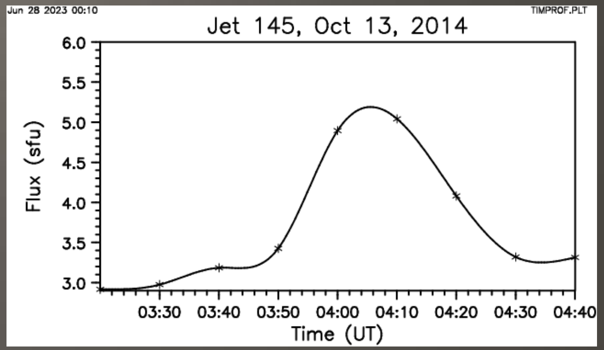

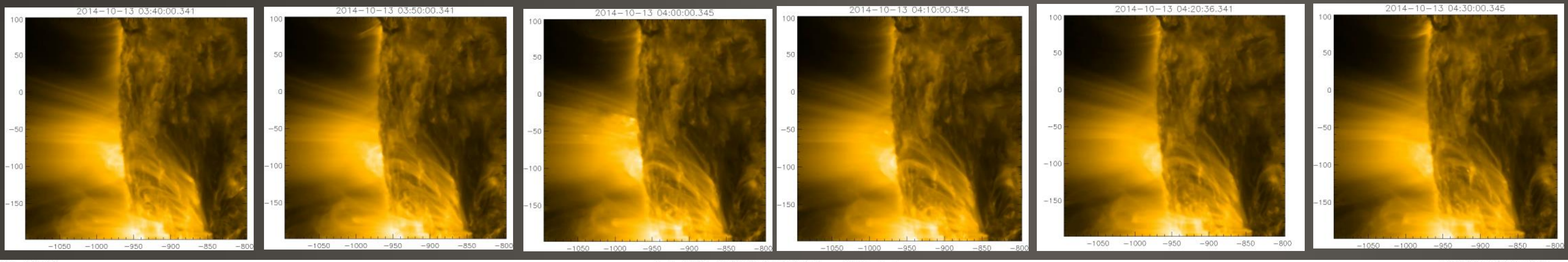

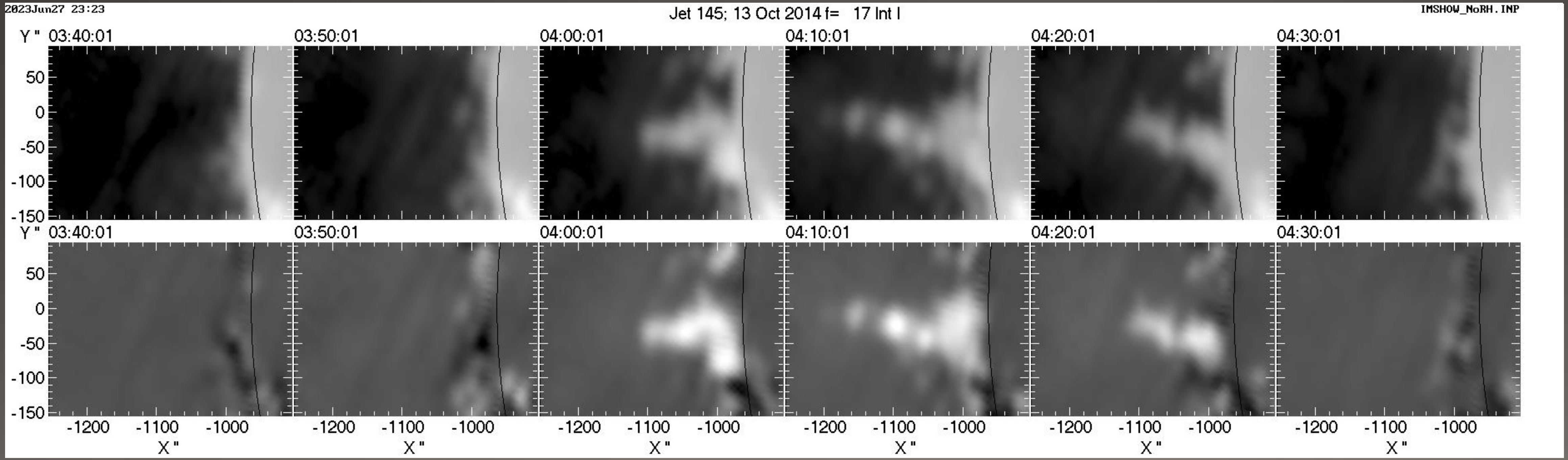

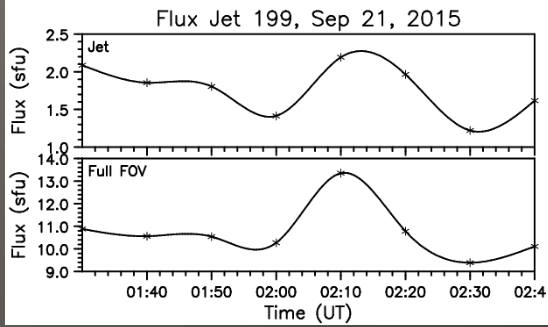

Kaltman 199, Sep 21, 2015

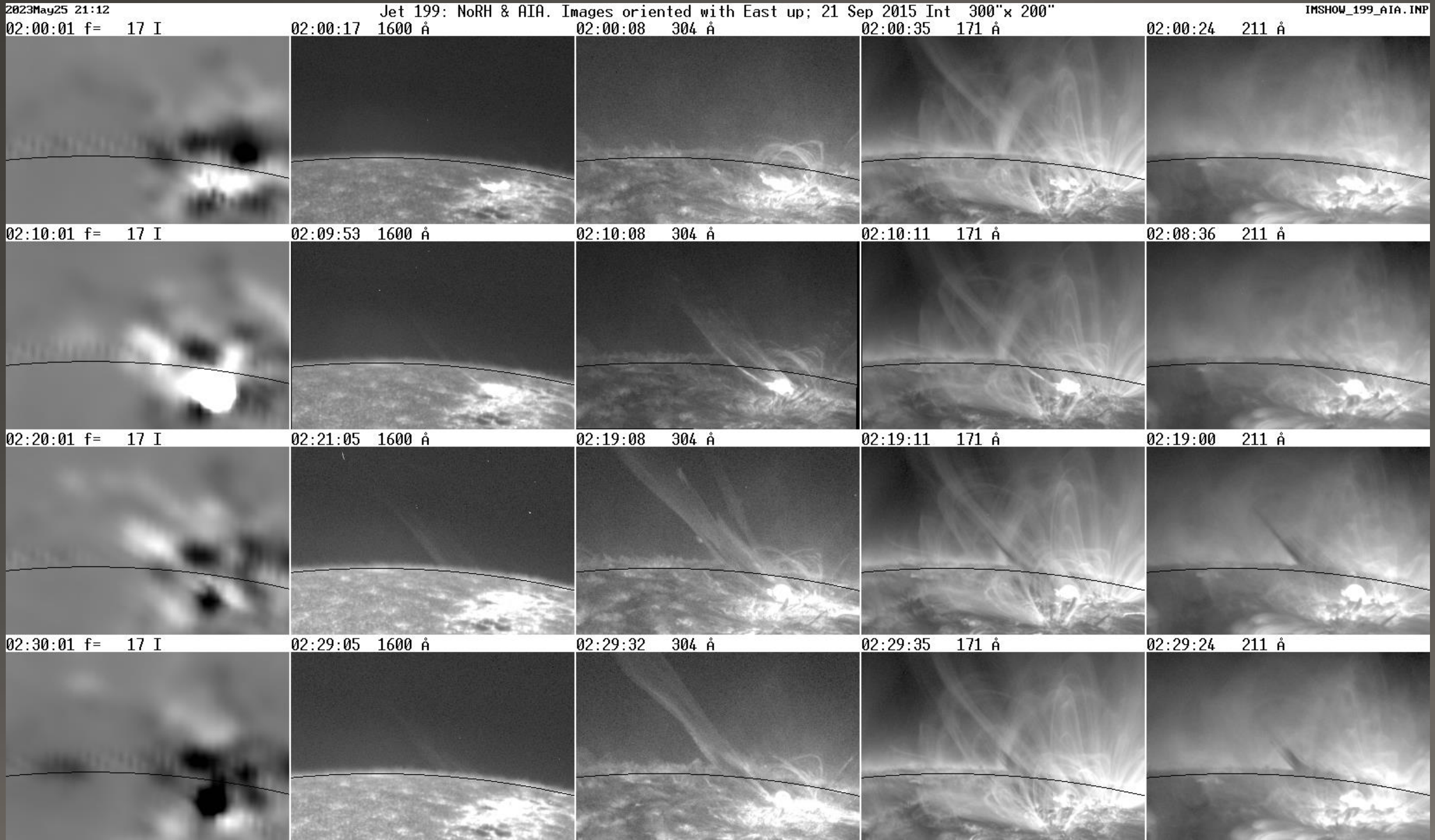

Event 368, Dec 26, 2017

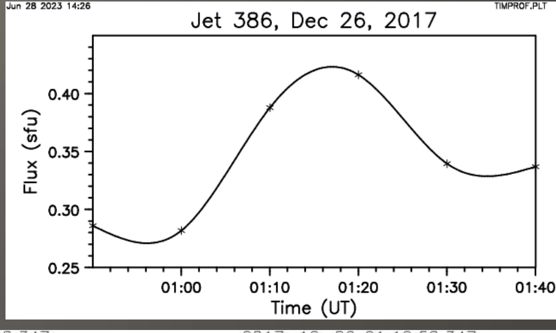

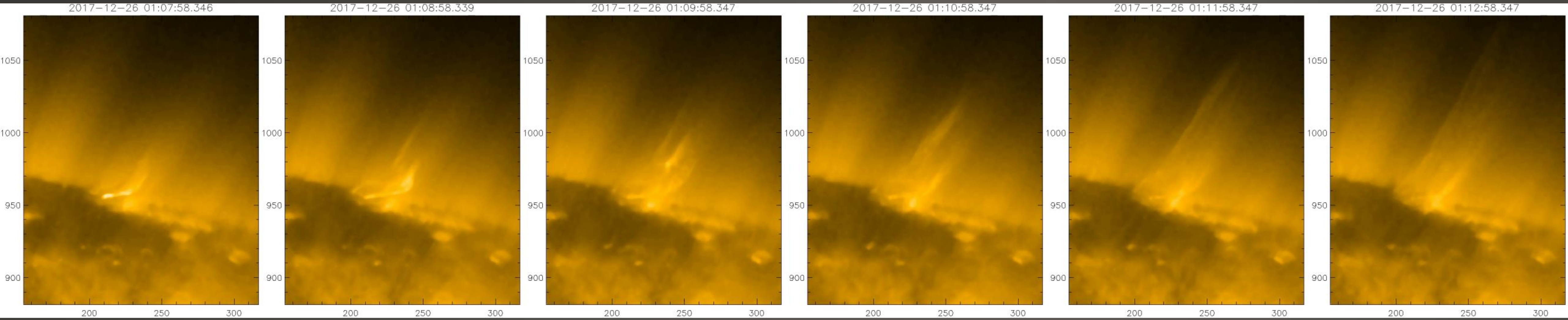

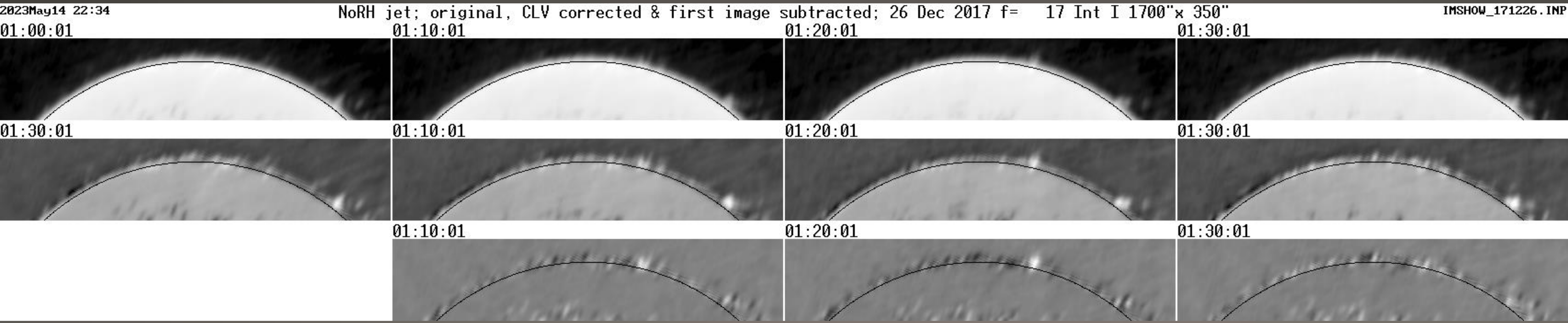

Kaltman 094, Dec 30, 2012

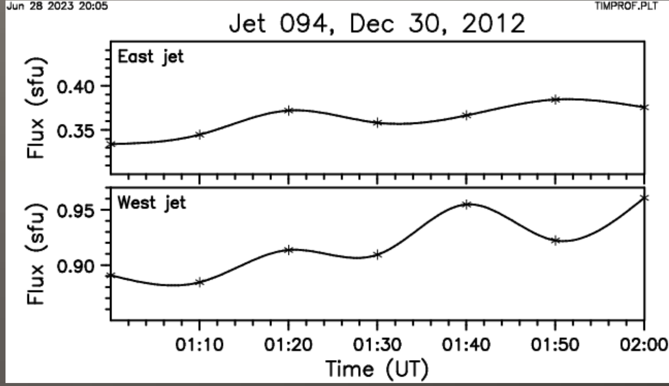

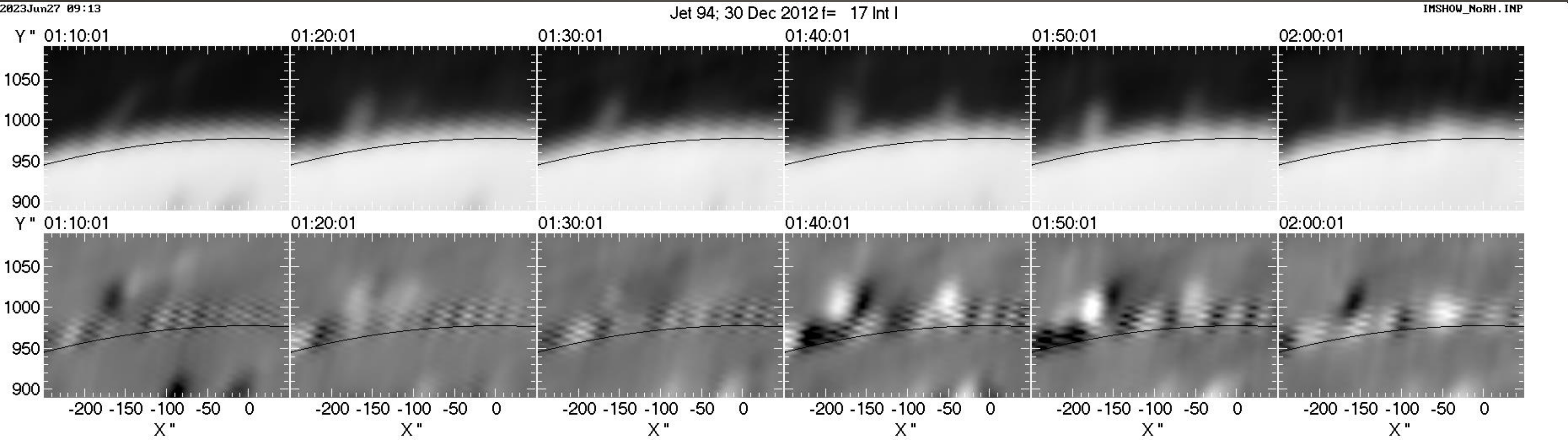

ALMA 100 GHz (3mm)

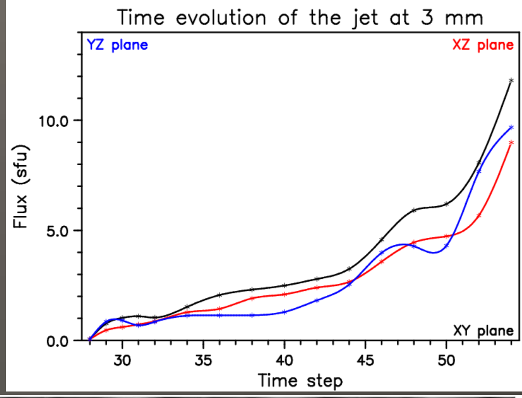

- Transient brightenings (Nindos et al, 2020 , 2021 ; Eklund et al., 2021)

(Nindos et al., 2021)

Parameter	Apr 2018 1.26mm	Apr 2018 3mm	Mar 2017 3mm
max intensity (K)	44-449	65-511	71-504
Mean area (Mm^2)	5.2	9.3	12.3
Mean duration (s)	50.7	49.7	51.1

(Nindos et al., 2021)

⇒ 3 mm flux for 500 K: 0.007 sfu (thin), 0.098 sfu (thick)

=> too low

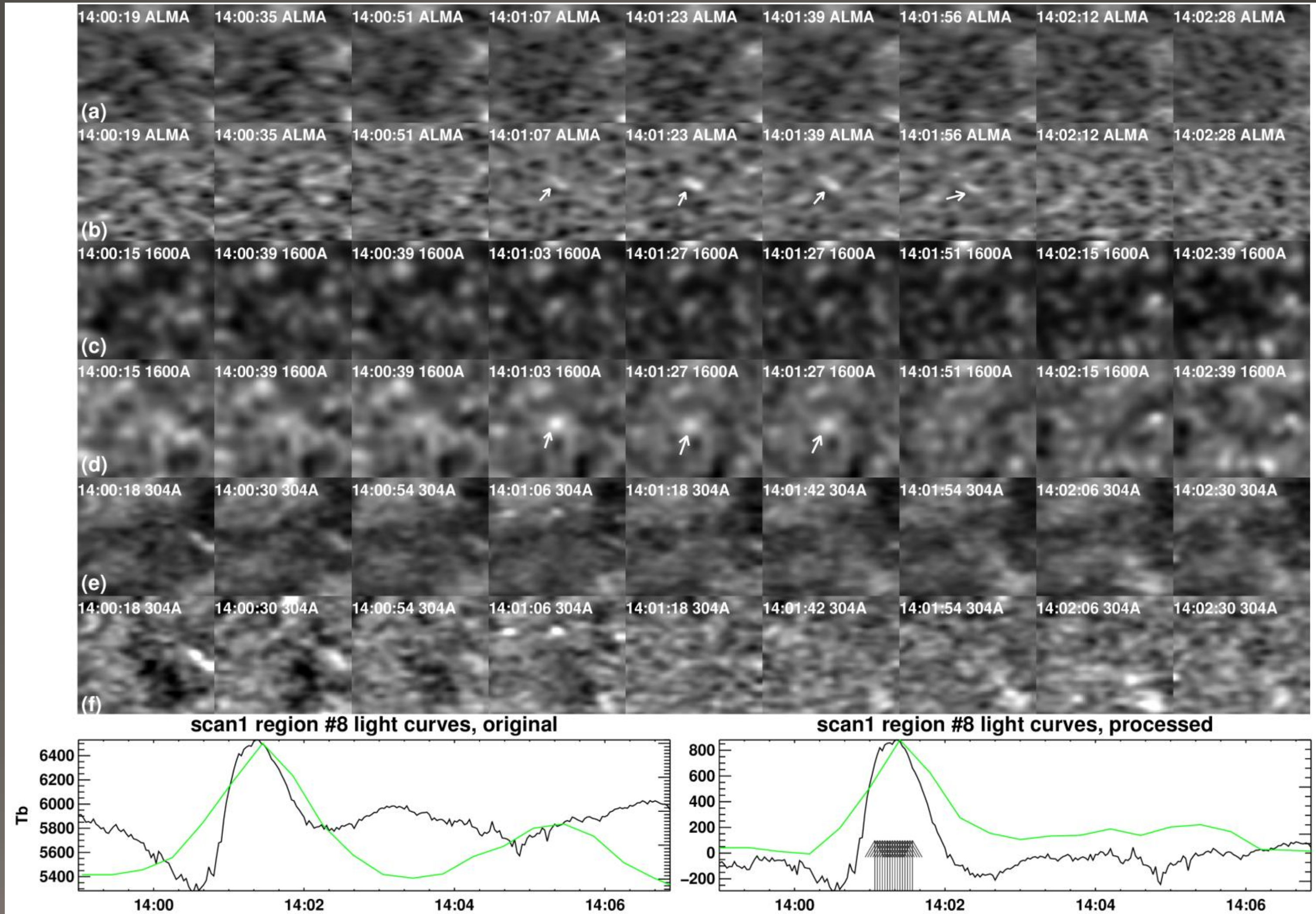

Shimojo et al. 2017 (plasmoid)

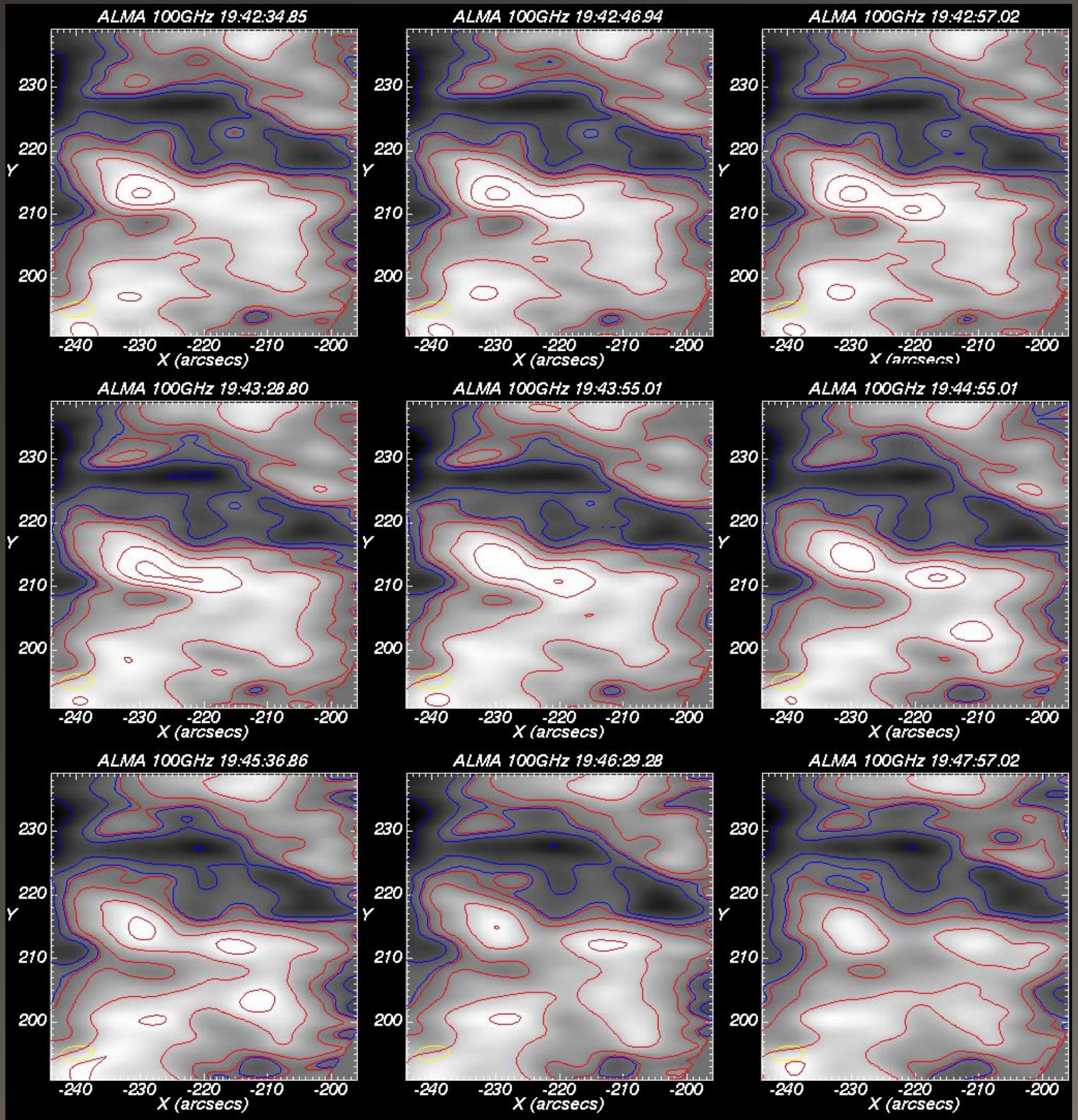

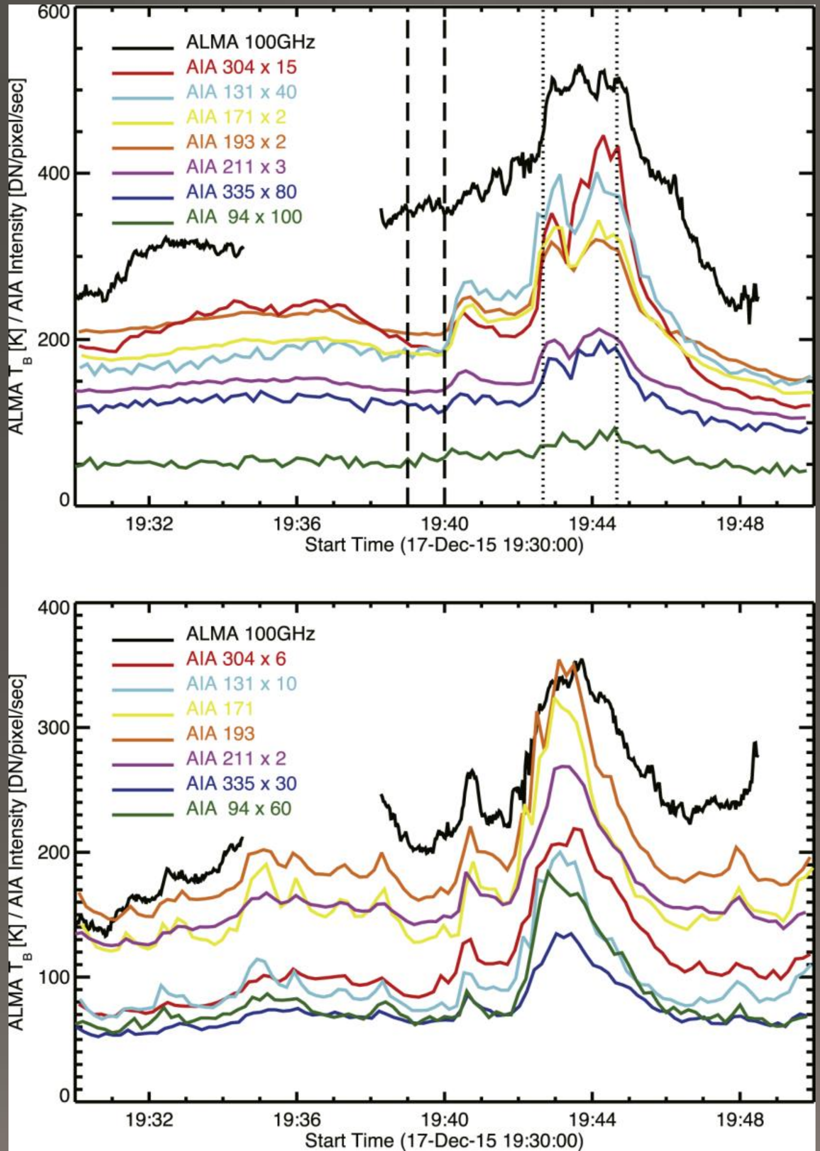

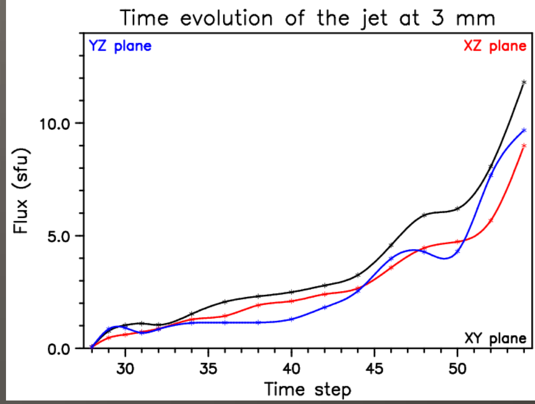

Flux ~ 1 sfu

Summary and conclusions

- The simulations predict things that look like jets
- Radio flux during the first phase at 17 GHz comparable to NoRH measurements
- At 100 GHz the predicted flux is well above that of transient brightenings, but comparable to that of a plasmoid ejection
- Predicted brightness in AIA EUV channels is above the observed (need to check further)

This work was supported in part by the ERC synergy grant 'The Whole Sun'

That’s all for the time being

- Stay tuned for more!

This work was supported in part by the ERC synergy grant 'The Whole Sun'